Broadband Terahertz Absorber Using Superimposed Graphene Quantum Dots

Hadi Deljoo
University of Tabriz
Ali Rostami (rostami@tabrizu.ac.ir)
University of Tabriz https://orcid.org/0000-0002-8727-4711

Research Article

Keywords: Broadband absorber, graphene, metamaterial.

Posted Date: February 17th, 2021

DOI: https://doi.org/10.21203/rs.3.rs-198205/v1

Version of Record: A version of this preprint was published at Optical and Quantum Electronics on July 22nd, 2021. See the published version at https://doi.org/10.1007/s11082-021-03116-2.

Broadband Terahertz Absorber using superimposed Graphene Quantum Dots

H. Deljo[1], and A. Rostami[1, 2]

[1]Photonics and Nanocrystal Research Lab. (PNRL), Faculty of Electrical and Computer Engineering, University of Tabriz, Tabriz 5166614761, Iran

[2]SP-EPT Lab., ASEPE Company, Industrial Park of Advanced Technologies, Tabriz 5169654916, Iran

Abstract— In this study, we propose and investigate numerically a broadband THz metamaterial-based absorber, which is composed of superimposed Graphene Quantum Dots. Based on this idea, a new way to engineering the absorption band is introduced. We will show that using the proposed idea, it is possible to design a THz absorber with a given bandwidth. To show the capability of the idea, we consider a three-layer structure, and the top layer is superimposed graphene disks. The middle layer is a lossless dielectric thin layer and eventually gold is placed in the bottom layer. Simulation results reveal a broadband absorption in the range of (5.86THz to 7.57THz), (5.89THz to 7.56THz), and (5.89THz to 7.58THz) while absorption values respectively are above 89%, 88.49%, and 88.32%. The dielectric material is Si_3N_4 in the proposed structure. Also, the broadband absorption range is 7.47THz to 9.87THz with an absorption value above 80% while the dielectric material is SiO_2.

Keywords— Broadband absorber, graphene, metamaterial.

I. INTRODUCTION

Metamaterials are artificial materials that are designed in periodic arrays. They have interesting electromagnetic properties, like negative refractive index [1], asymmetric transmission [2], and cross-polarization conversion [3]. Due to the above-mentioned properties metamaterials can become perfect choices for the electromagnetic absorber. Metamaterial absorber has been demonstrated for the first time by Landy et al in 2008 [4]. After that, different designs for metamaterial absorbers have been proposed in the electromagnetic spectral range including microwave [5], terahertz [6], infrared [7, 8], and optical frequency [9].

Terahertz technology is developing increasingly. Terahertz has interesting applications in information and communication technology, biomedical imaging, security, astronomy, and spectroscopy [10-15]. A little number of materials in nature can interact with Terahertz waves. Due to the lack of efficient Terahertz sources and detectors, working with Terahertz waves is still an enormous challenge [16]. By changing the size of the metamaterial structure they can easily respond to Terahertz waves. These structures have the limitation that when they are designed they can act only in a single frequency. Most of the absorbers have the limitation that they only can work at a single band to multi-band. Also, they have limitations in the frequency range. Broadband absorption has been the approach of different attempts in the last decade. Some works are fabricated or designed to reach broadband absorption in the visible [17-19], near-infrared [20, 21], mid-infrared [7, 22-24], and Terahertz [25-28] ranges. The tendency is towards designing structures with the ability of tunability so this requires new materials.

Graphene is a 2D nanomaterial, which consists of a single layer of carbon atoms that are arranged in a hexagonal lattice [29]. It has been applied in different optoelectronic applications due to its excellent properties such as optical transparency, flexibility [30] ultrahigh carrier mobility [31]. Its carrier mobility and conductivity can be tuned by applying an external electric field [32] or chemical doping [33] in the range of infrared to terahertz. This property caused graphene to be the most important candidate in perfect absorbers.

In this paper, we propose a broadband metamaterial terahertz absorber in the range of 5.86THz to 7.57THz), (5.89THz to 7.56THz), (5.89THz to 7.58THz), and (7.47THz to 9.87THz). This structure consists of 7 sets of disks with different radii located on a lossless dielectric thin layer and a metal film at the bottom.

II. STRUCTURE AND DESIGN

The proposed structure is demonstrated in Fig. 1. The absorber has three layers. A single layer of graphene disks (superimposed Graphene QDs) in 7 sets. The middle layer is Silicon Dioxide with its permittivity of 3.9. The thickness of the middle layer is 3.9 μm. The length of this layer is 29.4 μm and the width of this layer is 4.2 μm. We considered gold at the bottom layer which its electric conductivity $\sigma_{gold} = 4.56 \times 10^7\ {}^{S}/_{m}$. The thickness of this layer is 0.2 μm. The length of the gold layer is equal to 29.4 μm and the width is 4.2 μm. Each set of graphene disks has a specified radius. It means that in the first set the radius is equal to 400 nm, in the second set the radius is equal to 430 nm, in third 461 nm, in fourth 493 nm, in fifth 525 nm, in sixth 556 nm, and in the seventh set, the radius of disks is equal to 586 nm. Our structure is made up of putting 7 unit cells with a length of 4.2 μm and a width of 4.2 μm beside each other. In every set of graphene disks, one circle is located in the middle of the unit cell and the other 4 disks are located at the diagonals.

Interband and intraband contributions are considered for the surface conductivity of graphene regarding the Kubo formula [34, 35],

$$\sigma_S = \sigma_S^{intra} + \sigma_S^{inter} \quad (1)$$

$$\sigma_S^{intra} = \frac{2k_B T e^2}{\pi\bar{h}^2}\ln(2cosh\frac{E_F}{2k_B T})\frac{i}{\omega+i\tau^{-1}} \quad (2)$$

$$\sigma_S^{inter} = \frac{e^2}{4\bar{h}}[H\left(\frac{\omega}{2}\right) + i\ \frac{4\omega}{\pi}\int_0^{\infty}\frac{H(\Omega)-H(\frac{\omega}{2})}{\omega^2-4\Omega^2}d\Omega] \quad (3)$$

Where $H(\Omega) = \sinh\left(\frac{\bar{h}\Omega}{k_B T}\right)/[\cosh\left(\frac{\bar{h}\Omega}{k_B T}\right) + \cosh\left(\frac{E_F}{k_B T}\right)]$, T is the temperature, E_F is electrochemical potential (Fermi energy), ω is the frequency of the electromagnetic wave and τ is relaxation time and e is the charge of an electron. In THz range, because photon energy $\bar{h}\omega \ll E_F$, so we can neglect the interband part in comparison with the intraband part. As a result, the surface conductivity of graphene in the THz range can be described by the Drude model [36]:

$$\sigma_g(\omega) = \frac{e^2 E_f}{\pi\bar{h}^2}\frac{i}{\omega+i\tau^{-1}} \quad (4)$$

At a specified E_f, graphene conductivity changes by changing frequency. whereas an imaginary part of the graphene conductivity determines resonance spectral shift and the real part of graphene conductivity determines resonance amplitude modulation, by applying an external electric field or using an optical pump we can tune the absorption by controlling the Fermi level.

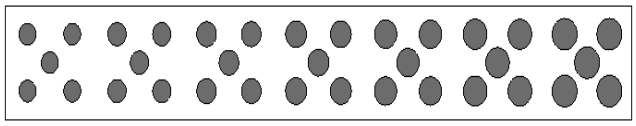

(a)

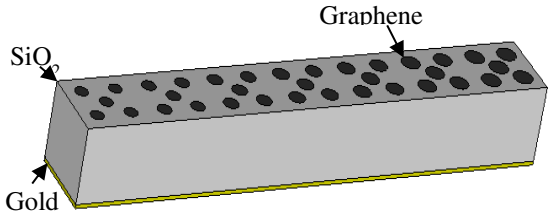

(b)

Fig. 1. (a) 7 sets of 5 disks. In 1st set, the radius is 400nm. In 2nd is 431nm. In 3rd is 461nm. In 4th is 493nm. In 5th is 525nm. In 6th is 556nm. In 7th is 586nm. (b) Schematic illustration of proposed THz metamaterial absorber. The top layer is composed of graphene disks. The middle layer is SiO_2 and the bottom layer is gold.

The proposed structure is illuminated by the TE wave in which propagation direction is along the z-direction. CST Microwave Studio commercial software was used in this study to carry out numerical simulations. Unit cell boundary conditions were applied in x and y directions. Open space boundary conditions were used in the z-direction. Absorption can be calculated using $A(\omega) = 1 - |S_{11}|^2 - |S_{21}|^2$, where S_{11} and S_{21} are reflection and transmission coefficients respectively. These parameters can be acquired from CST simulation results. Because the thickness of the bottom metallic layer is thicker than the skin depth at frequencies that we carry out our study, approximately no electromagnetic wave penetrates the structure. So we can suppose $S_{21} = 0$, then $A(\omega) = 1 - |S_{11}|^2$.

III. Results and Discussion

Our goal is to design a broadband THz detector. To this end, first of all, we must find a unit cell structure with maximum absorption, then putting together these unit cells beside each other we expect to design a structure with broadband detection. We have used the TE wave to study the proposed absorber. We have supposed Fermi energy of graphene as $E_f = 0.6eV$ and relaxation time is $\tau = 0.5ps$. To approach the best result, first of all, we should find the unit cell structure with maximum absorption. Then putting together these unit cells we want to find the structure with broadband absorption. According to [29] we have supposed unit cells with three layers. The bottom layer is composed of gold with a height of 200nm, the middle layer is SiO_2 with a height of 3900nm and the top layer is composed of 5 disks of single-layer graphene as Fig. 2.

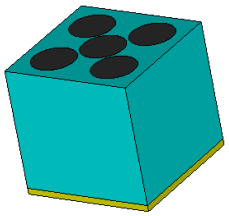

Fig. 2. Unit cell with 5 disks of single-layer graphene at top. The middle layer is SiO_2 and the bottom layer is gold.

The results of the graphene disk's radius sweep from 300 to 700 are demonstrated in Fig. 3. In Fig. 3. Maximum absorption is occurred with radius=350nm, at the frequency of 11.25 THz with an absorption value of 99.96%. The results for gold layer height sweep from 40nm to 320nm with the step of 40nm are shown in Fig. 4.

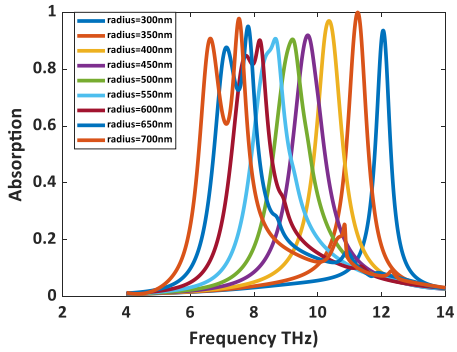

Fig. 3. Radius sweep from 300 to 700.

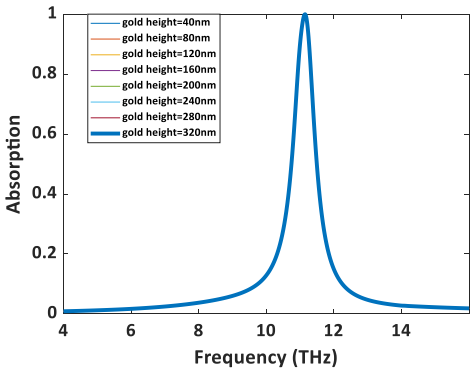

Fig. 4. Gold layer height sweep from 40nm to 320nm.

Fig. 4 shows that gold layer height has not any effect on absorption value. Sweeping the height of the SiO_2 layer from 300 to 4500nm with a step of 300nm, the results are given in Fig. 5.

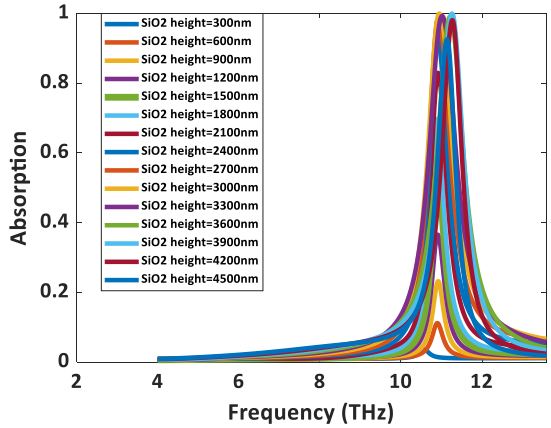

Fig. 5. SiO_2 layer height sweep from 300nm to 4500nm.

According to the above figure, in the height of SiO_2 layer=3900nm, maximum absorption occurs with a value of 99.99% in 11.25 THz. Sweeping the dimension of the unit cell from 600nm to 5400nm, the following result is acquired.

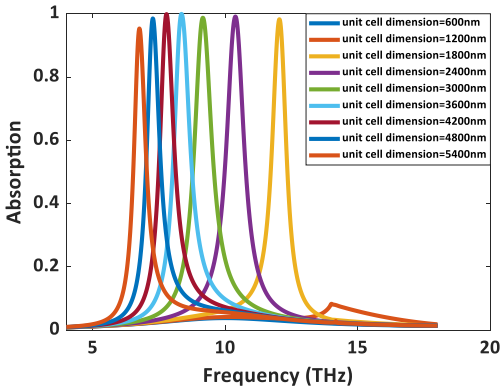

Fig. 6. Sweeping the dimension of the unit cell from 600 to 5400nm.

In Fig. 6. the maximum absorption value is 99.94% in the frequency of 8.34THz with the dimension of unit cell=3600nm. The results of sweeping the dimension of the unit cell from 700nm to 5600nm can be shown in Fig. 7.

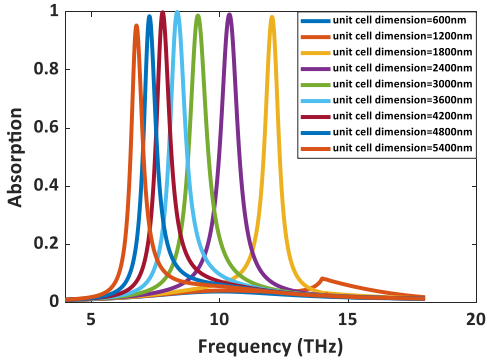

Fig. 7. Sweeping the dimension of the unit cell from 700 to 5600nm.

In the above figure, the maximum absorption value is 99.96% in the frequency of 10.96THz with the dimension of unit cell=2100nm. Sweeping the dimension of the unit cell from 800nm to 5600nm the results can be demonstrated in the following figure.

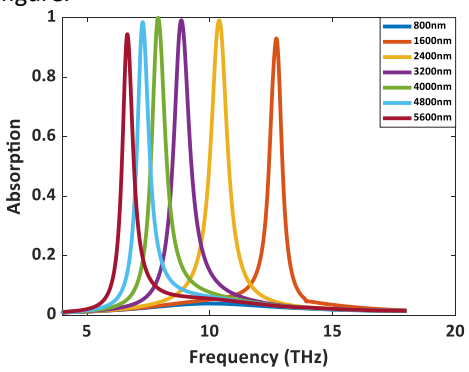

Fig. 8. Sweeping the dimension of the unit cell from 800 to 5600nm.

The maximum absorption value is 99.95% in the frequency of 7.89THz with the dimension of unit cell=4000nm. We have located one of five circles in (0,0), and located the other four circles in (x,y), (x,-y), (-x,y), (-x,-y). We considered x=y. Sweeping x and y from 500nm to 1750nm results are denoted in Fig. 9.

Maximum absorption value is 99.99% when (x,y)=(1050,1050). Due to above sweeps maximum absorption with the value of 99.99% occurs when the dimension of unit cell=2100nm, gold layer height=240nm, SiO_2 layer height=3900nm, location of five disks of graphene are (-1050,-1050), (-1050,1050), (0,0), (1050, -1050), (1050,1050). As previously mentioned we have designed a structure with maximum absorption, then our policy is to locate these structures beside each other and then find a structure with broadband detection, so we put three unit cells beside each other to find the structure with broadband THz detection as Fig. 10.

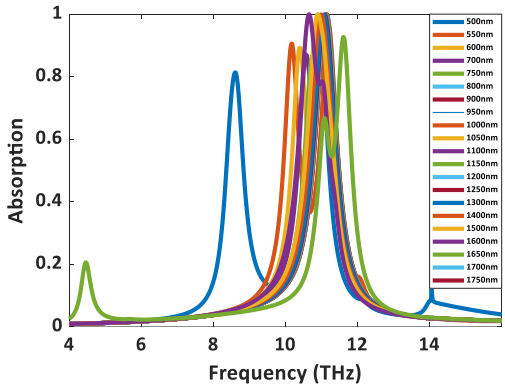

Fig. 9. Sweeping the location of disks from 500 to 1750nm.

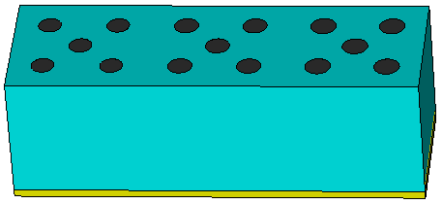

Fig.10. putting 3 unit cells beside each other.

We have assumed radii of disks in the first unit cell as 350, in the second unit cell as 370, and the third unit cell as 390. We have allocated different materials for the middle layer in Fig. 10. We have considered dielectric constant= 3.1, 3.3, 3.5, 3.7, 3.9 respectively for Rubber, Zircon, Polyimide, Quartz, SiO_2. The result is depicted in Fig. 11.

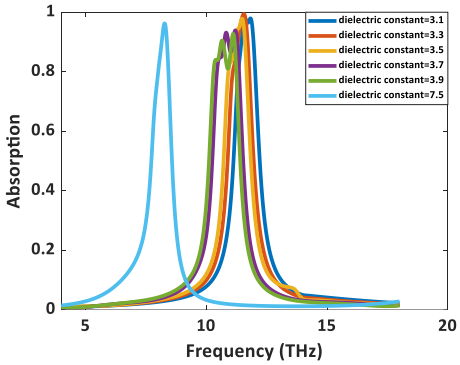

Fig.11. Radii of graphene disks in first unit cell=350nm, second=370nm, and third=390nm with middle layer dielectric constant=3.1 (Rubber), 3.3 (Zircon), 3.5 (Polyimide), 3.7 (Quartz), 3.9 (SiO_2), and 7.5 (Si_3N_4).

We have assumed radii of disks in the first unit cell as 350, in the second unit cell as 375, and the third unit cell as 400. We have allocated different materials for the middle layer in Fig. 10. We have considered dielectric constant= 3.1, 3.3, 3.5, 3.7, 3.9 respectively for Rubber, Zircon, Polyimide, Quartz, SiO_2. The result is demonstrated in Fig. 12.

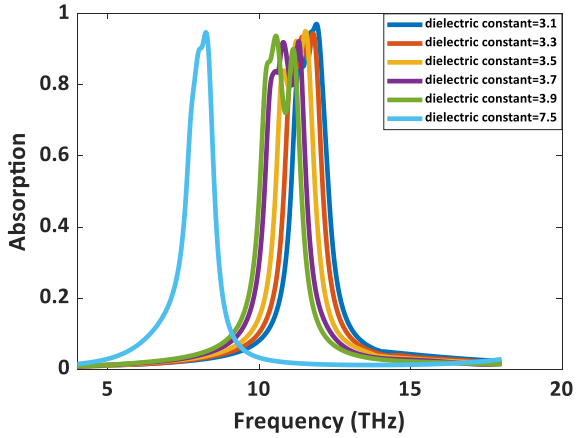

Fig.12. Radii of graphene disks in first unit cell=350nm, second=375nm, and third=400nm with middle layer dielectric constant=3.1 (Rubber), 3.3 (Zircon), 3.5 (Polyimide), 3.7 (Quartz), 3.9 (SiO_2), and 7.5 (Si_3N_4).

We have assumed radii of disks in the first unit cell as 350, in the second unit cell as 380, and the third unit cell as 410. We have allocated different materials for the middle layer in Fig. 10. We have considered dielectric constant= 3.1, 3.3, 3.5, 3.7, 3.9 respectively for Rubber, Zircon, Polyimide, Quartz, SiO_2. The result is demonstrated in Fig. 13.

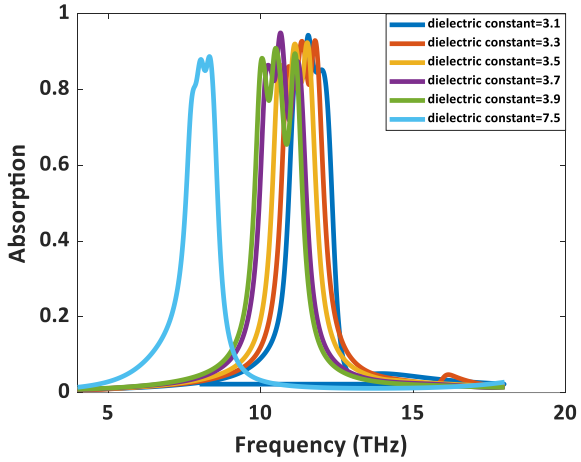

Fig.13. Radii of graphene disks in first unit cell=350nm, second=375nm, and third=400nm with middle layer dielectric constant=3.1 (Rubber), 3.3 (Zircon), 3.5 (Polyimide), 3.7 (Quartz), 3.9 (SiO_2), and 7.5 (Si_3N_4).

Using 3 unit cells has not satisfied us in approaching a broadband THz detector. So we decide to put 5 unit cells beside each other and verify the results.

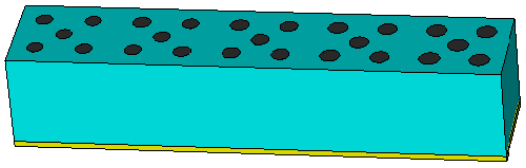

Fig.14. putting 5 unit cells beside each other.

We assumed radii of disks in the first unit cell as 350, in the second unit cell as 370, and the third unit cell as 390, in the

fourth unit cell as 410, and finally in the fifth unit cell as 430. Also, we have considered different materials for the middle layer in Fig. 14. The dedicated dielectric constants are as following: 3.1, 3.3, 3.5, 3.7, 3.9 respectively for Rubber, Zircon, Polyimide, Quartz, SiO_2. The results are given in Fig. 15.

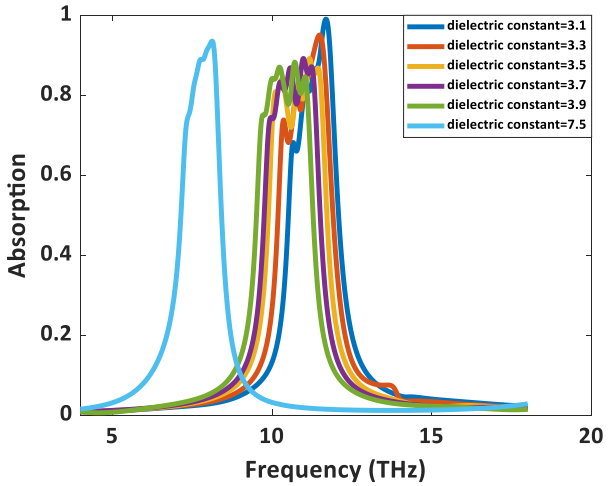

Fig.15. Radii of graphene disks in first unit cell=350nm, second=370nm third=390nm, fourth=410nm and fifth=430nm with middle layer dielectric constant=3.1 (Rubber), 3.3 (Zircon), 3.5 (Polyimide), 3.7 (Quartz), 3.9 (SiO_2) and 7.5 (Si_3N_4).

We assumed radii of disks in the first unit cell as 350, in the second unit cell as 375 and the third unit cell as 400, in the fourth unit cell as 425, and finally in the fifth unit cell as 450. Also, we have considered different materials for the middle layer in Fig. 14. The results are depicted in Fig. 16.

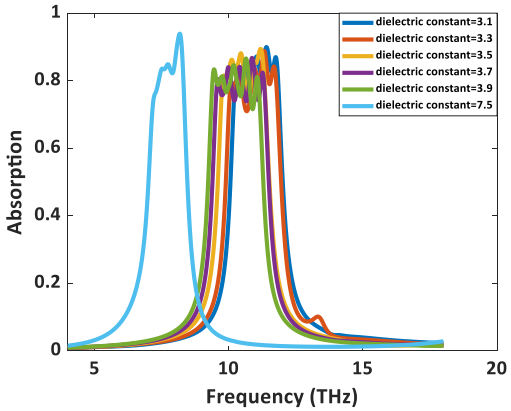

Fig.16. Radii of graphene disks in first unit cell=350nm, second=375nm third=400nm, fourth=425nm and fifth=450nm with middle layer dielectric constant=3.1 (Rubber), 3.3 (Zircon), 3.5 (Polyimide), 3.7 (Quartz), 3.9 (SiO_2) and 7.5 (Si_3N_4).

We assumed radii of disks in the first unit cell as 350, in the second unit cell as 380, and the third unit cell as 410, in the fourth unit cell as 440, and finally in the fifth unit cell as 470. Also, we have considered different materials for the middle layer in Fig. 14. The results are depicted in Fig. 17.

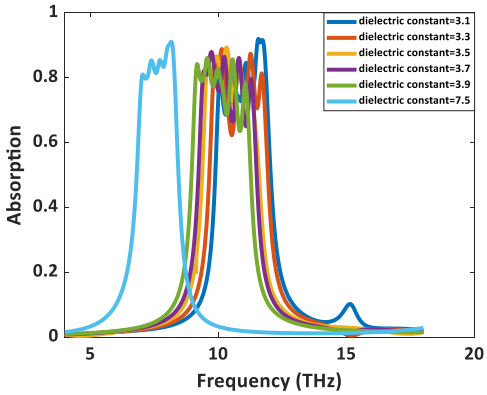

Fig.17. Radii of graphene disks in first unit cell=350nm, second=380nm third=410nm, fourth=440nm and fifth=470nm with middle layer dielectric constant=3.1 (Rubber), 3.3 (Zircon), 3.5 (Polyimide), 3.7 (Quartz), 3.9 (SiO_2) and 7.5 (Si_3N_4).

Referring to fig. 17. We can conclude that continuing the process of placing unit cells beside each other will improve the output waveform to achieve broadband detection, so we put 7 unit cells beside each other and continue the simulation process.

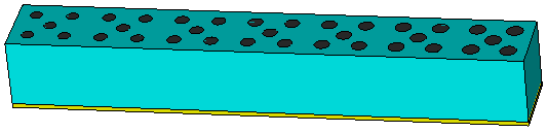

Fig.18. putting 5 unit cells beside each other.

Putting 7 unit cells beside each other, we assumed radii of disks in the first unit cell as 350, in the second unit cell as 370 and the third unit cell as 390, in the fourth unit cell as 410, in the fifth unit cell as 430, in sixth unit cell 450 and finally in seventh unit cell as 470. Also, we have considered different materials for the middle layer in Fig. 18 like previous figures. The results are demonstrated in Fig. 19.

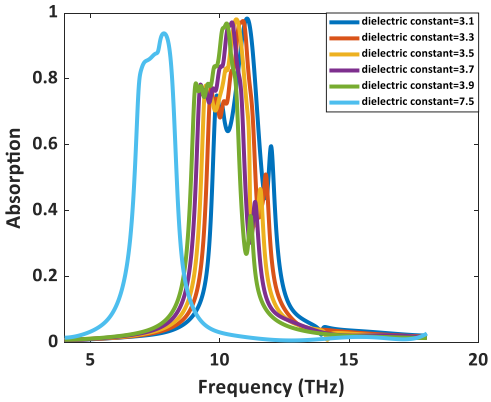

Fig.19. Radii of graphene disks in first unit cell=350nm, second=370nm third=390nm, fourth=410nm, fifth=430nm, sixth=450 and seventh=470 with middle layer dielectric constant=3.1 (Rubber), 3.3 (Zircon), 3.5 (Polyimide), 3.7 (Quartz), 3.9 (SiO_2) and 7.5 (Si_3N_4).

We assumed radii of disks in the first unit cell as 350, in second unit cell as 375 and third unit cell as 400, in the fourth unit cell as 425, in fifth unit cell as 450, in sixth unit cell 475, and finally

in seventh unit cell as 500. Also, we have considered different materials for the middle layer in Fig. 18 like previous figures. The results are demonstrated in Fig. 20.

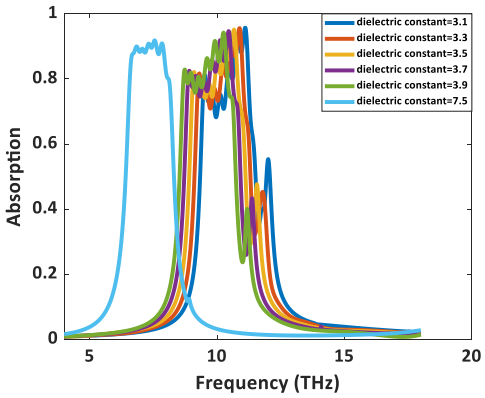

Fig.20. Radii of graphene disks in first unit cell=350nm, second=375nm third=400nm, fourth=425nm, fifth=450nm, sixth=475 and seventh=500 with middle layer dielectric constant=3.1 (Rubber), 3.3 (Zircon), 3.5 (Polyimide), 3.7 (Quartz), 3.9 (SiO_2) and 7.5 (Si_3N_4).

We assumed radii of disks in the first unit cell as 350, in second unit cell as 380, and third unit cell as 410, in the fourth unit cell as 440, in fifth unit cell as 470, in sixth unit cell 500, and finally in seventh unit cell as 530. Also, we have considered different materials for the middle layer in Fig. 18 like previous figures. The results are demonstrated in Fig. 21.

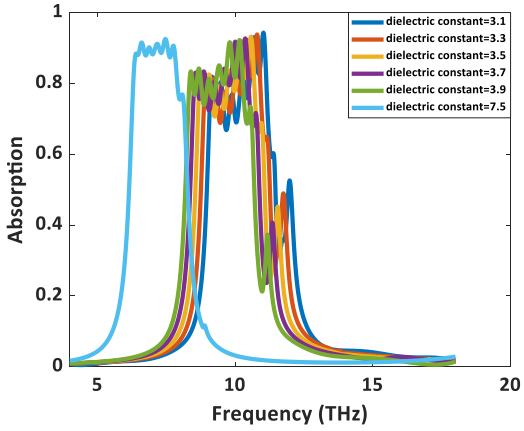

Fig.21. Radii of graphene disks in first unit cell=350nm, second=380nm third=410nm, fourth=440nm, fifth=470nm, sixth=500 and seventh=530 with middle layer dielectric constant=3.1 (Rubber), 3.3 (Zircon), 3.5 (Polyimide), 3.7 (Quartz), 3.9 (SiO_2) and 7.5 (Si_3N_4).

We assumed radii of disks in the first unit cell as 350, in second unit cell as 385 and third unit cell as 420, in the fourth unit cell as 455, in fifth unit cell as 490, in sixth unit cell 525, and finally in seventh unit cell as 560. Also, we have considered different materials for the middle layer in Fig. 18 like previous figures. The results are demonstrated in Fig. 22.

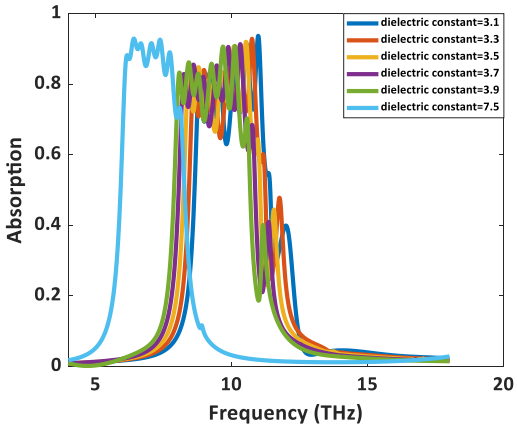

Fig. 22. Radii of graphene disks in first unit cell=350nm, second=385nm third=420nm, fourth=455nm, fifth=490nm, sixth=525 and seventh=560 with middle layer dielectric constant=3.1 (Rubber), 3.3 (Zircon), 3.5 (Polyimide), 3.7 (Quartz), 3.9 (SiO_2) and 7.5 (Si_3N_4).

In the following figures, we have depicted results with different radii of disks in 7 unit cells to compare them and result in the best condition for the THz broadband detector.

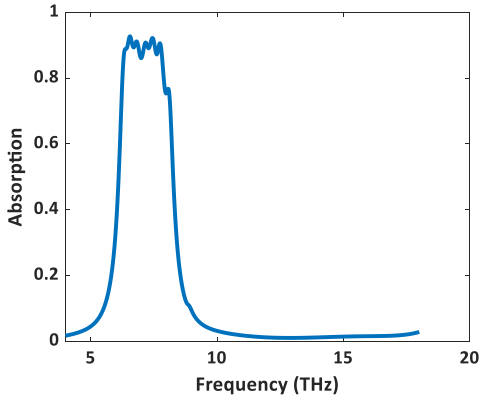

Fig.23. Radii of graphene disks in first unit cell=350nm, second=380nm third=411nm, fourth=443nm, fifth=475nm, sixth=506 and seventh=536 with middle layer dielectric constant= 7.5 (Si_3N_4).

Table 1. The mathematical relation between radii of 5 graphene disks in 7 unit cells that are put beside each other in Fig. 23.

Unit cell	Radius (nm)	**Added amount to the previous unit cell radius**
1st unit cell	350	0
2nd unit cell	380	30
3rd unit cell	411	31
4th unit cell	443	32
5th unit cell	475	32
6th unit cell	506	31
7th unit cell	536	30

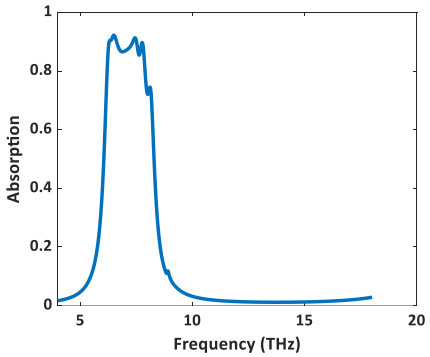

Fig. 24. Radii of graphene disks in first unit cell=350nm, second=380nm third=412nm, fourth=446nm, fifth=480nm, sixth=512 and seventh=542 with middle layer dielectric constant= 7.5 (Si_3N_4).

Table 2. The mathematical relation between radii of 5 graphene disks in 7 unit cells that are put beside each other in Fig. 24.

Unit cell	Radius (nm)	**Added amount to the previous unit cell radius**
1st unit cell	350	0
2nd unit cell	380	30
3rd unit cell	412	32
4th unit cell	446	34
5th unit cell	480	34
6th unit cell	512	32
7th unit cell	542	30

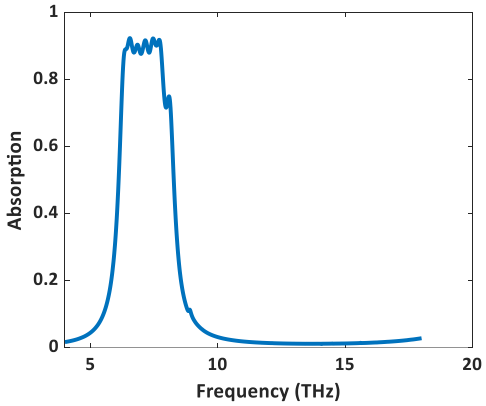

Fig.25. Radii of graphene disks in first unit cell=350nm, second=381nm third=412nm, fourth=443nm, fifth=474nm, sixth=505 and seventh=536 with middle layer dielectric constant= 7.5 (Si_3N_4).

Table 3. The mathematical relation between radii of 5 graphene disks in 7 unit cells that are put beside each other in Fig. 25.

Unit cell	Radius (nm)	**Added amount to the previous unit cell radius**
1st unit cell	350	0
2nd unit cell	381	31
3rd unit cell	412	31
4th unit cell	443	31
5th unit cell	474	31
6th unit cell	505	31
7th unit cell	536	31

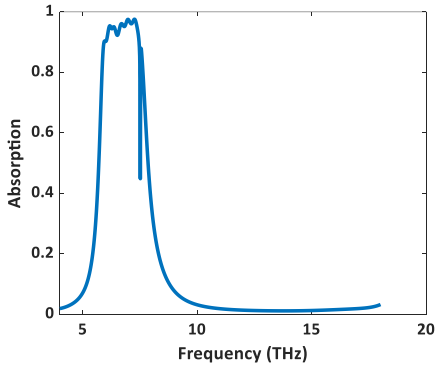

Fig.26. Radii of graphene disks in first unit cell=400nm, second=430nm third=461nm, fourth=493nm, fifth=525nm, sixth=556 and seventh=586 with middle layer dielectric constant= 7.5 (Si_3N_4).

Table 4. The mathematical relation between radii of 5 graphene disks in 7 unit cells that are put beside each other in Fig. 26.

Unit cell	Radius (nm)	**Added amount to the previous unit cell radius**
1st unit cell	400	
2nd unit cell	430	30
3rd unit cell	461	31
4th unit cell	493	32
5th unit cell	525	32
6th unit cell	556	31
7th unit cell	586	30

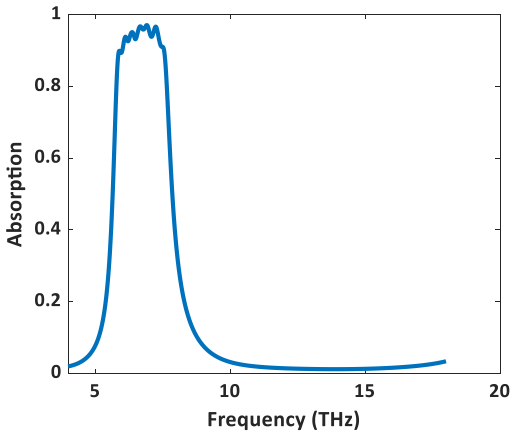

Fig. 27. Radii of graphene disks in first unit cell=400nm, second=431nm third=463nm, fourth=496nm, fifth=529nm, sixth=561 and seventh=592 with middle layer dielectric constant= 7.5 (Si_3N_4).

Table 5. The mathematical relation between radii of 5 graphene disks in 7 unit cells that are put beside each other in Fig. 27.

Unit cell	Radius (nm)	**Added amount to the previous unit cell radius**
1st unit cell	400	0
2nd unit cell	431	31
3rd unit cell	463	32
4th unit cell	496	33
5th unit cell	529	33
6th unit cell	561	32
7th unit cell	592	31

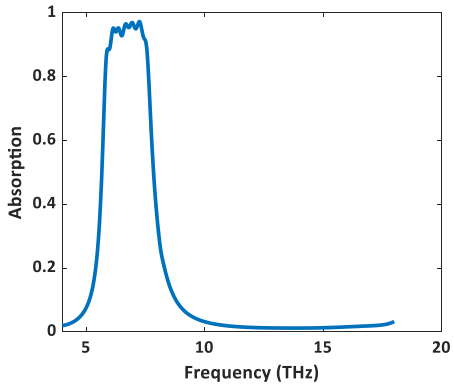

Fig.28. Radii of graphene disks in first unit cell=400nm, second=431nm third=463nm, fourth=495nm, fifth=527nm, sixth=559 and seventh=590 with middle layer dielectric constant= 7.5 (Si_3N_4).

Table 5. The mathematical relation between radii of 5 graphene disks in 7 unit cells that are put beside each other in Fig. 28.

Unit cell	Radius (nm)	**Added amount to the previous unit cell radius**
1st unit cell	400	0
2nd unit cell	431	31
3rd unit cell	463	32
4th unit cell	495	32
5th unit cell	527	32
6th unit cell	559	32
7th unit cell	590	31

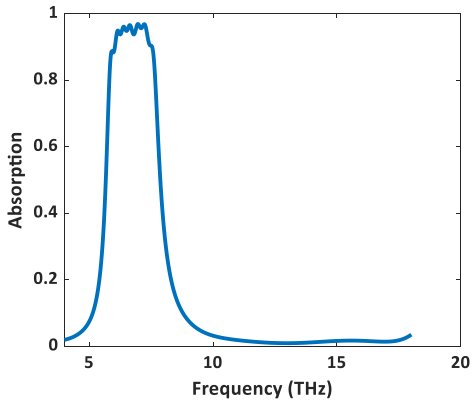

Fig. 29. Radii of graphene disks in first unit cell=400nm, second=431nm third=463nm, fourth=495nm, fifth=526nm, sixth=558 and seventh=590 with middle layer dielectric constant= 7.5 (Si_3N_4).

Table 6. The mathematical relation between radii of 5 graphene disks in 7 unit cells that are put beside each other in Fig. 29.

Unit cell	Radius (nm)	**Added amount to the previous unit cell radius**
1st unit cell	400	0
2nd unit cell	431	31
3rd unit cell	463	32
4th unit cell	495	32
5th unit cell	526	31
6th unit cell	558	32
7th unit cell	590	32

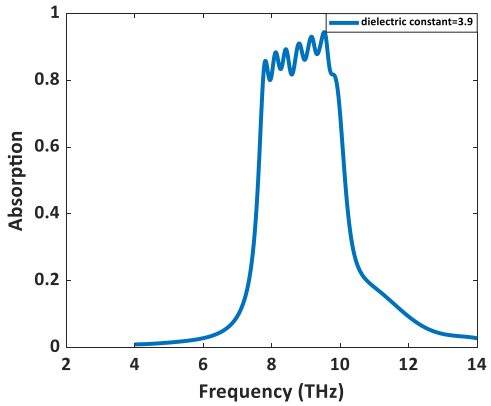

Fig.30. Radii of graphene disks in first unit cell=400nm, second=430nm third=461nm, fourth=493nm, fifth=525nm, sixth=556 and seventh=586 with middle layer dielectric constant= 3.9 (SiO_2).

Table 7. The mathematical relation between radii of 5 graphene disks in 7 unit cells that are put beside each other in Fig. 30.

Unit cell	Radius (nm)	**Added amount to the previous unit cell radius**
1st unit cell	400	0
2nd unit cell	430	30
3rd unit cell	461	31
4th unit cell	493	32
5th unit cell	526	32
6th unit cell	556	31
7th unit cell	586	30

IV. Conclusion

In summary, a broadband graphene-based metamaterial absorber was designed and investigated. The structure is composed of graphene disks at the top layer, the dielectric material in the middle layer, and a gold layer at the bottom. Simulation results reveal broadband absorption in the range of (5.86THz to 7.57THz) while maximum absorption value is 97.1% in the frequency of 6.91THz, in the range of (5.89THz to 7.56THz) while maximum absorption value is 97.3% in the frequency of 7.24THz and the range of (5.89THz to 7.58THz) while maximum absorption value is 96.91% in the frequency of 6.96THz. Absorption values respectively are above 89%, 88.49%, and 88.32% in the above-mentioned ranges and the middle dielectric material is Si_3N_4. The broadband absorption range is 7.47THz to 9.87THz with an absorption value above 80% while the dielectric material is SiO_2. The max absorption value is 94.46% in the frequency of 6.52THz in this range.

References

1. Pendry, J.B., Negative refraction. Contemporary Physics, 2004. 45(3): p. 191-202.
2. Xiao, Z.-y., et al., Multi-band transmissions of chiral metamaterials based on Fabry-Perot-like resonators. Optics Express, 2015. 23(6): p. 7053-7061.
3. Tang, J., et al., Cross polarization conversion based on a new chiral spiral slot structure in THz region. Optical and Quantum Electronics, 2016. 48(2): p. 111.
4. Landy, N.I., et al., Perfect metamaterial absorber. Physical review letters, 2008. 100(20): p. 207402.

5. Wu, B., et al., Experimental demonstration of a transparent graphene millimeter wave absorber with 28% fractional bandwidth at 140 GHz. Scientific reports, 2014. 4: p. 4130.
6. Liu, X., et al., Experimental realization of a terahertz all-dielectric metasurface absorber. Optics express, 2017. 25(1): p. 191-201.
7. Guo, W., Y. Liu, and T. Han, Ultra-broadband infrared metasurface absorber. Optics Express, 2016. 24(18): p. 20586-20592.
8. Zhong, Y.K., et al., Polarization-selective ultra-broadband super absorber. Optics express, 2017. 25(4): p. A124-A133.
9. Lin, C.-H., R.-L. Chern, and H.-Y. Lin, Polarization-independent broad-band nearly perfect absorbers in the visible regime. Optics express, 2011. 19(2): p. 415-424.
10. Chen, H.-T., et al., A metamaterial solid-state terahertz phase modulator. Nature Photonics, 2009. 3(3): p. 148-151.
11. Jansen, C., et al., Terahertz imaging: applications and perspectives. Applied optics, 2010. 49(19): p. E48-E57.
12. Jepsen, P.U., D.G. Cooke, and M. Koch, Terahertz spectroscopy and imaging–Modern techniques and applications. Laser & Photonics Reviews, 2011. 5(1): p. 124-166.
13. Saeedkia, D., et al., Analysis and design of a photoconductive integrated photo mixer/antenna for terahertz applications. IEEE journal of quantum electronics, 2005. 41(2): p. 234-241.
14. Tonouchi, M., Cutting-edge terahertz technology. Nature Photonics, 2007. 1(2): p. 97.
15. Williams, G.P., Filling the THz gap—high power sources and applications. Reports on Progress in Physics, 2005. 69(2): p. 301.
16. Ma, Y., et al., A terahertz polarization insensitive dual-band metamaterial absorber. Optics Letters, 2011. 36(6): p. 945-947.
17. Dorche, A.E., et al., Broadband, polarization-insensitive, and wide-angle optical absorber based on fractal plasmonics. IEEE Photonics Technology Letters, 2016. 28(22): p. 2545-2548.
18. Ghobadi, A., et al., Visible light nearly perfect absorber: an optimum unit cell arrangement for near absolute polarization insensitivity. Optics express, 2017. 25(22): p. 27624-27634.
19. Hubarevich, A., et al., Ultra-thin broadband nanostructured insulator-metal-insulator-metal plasmonic light absorber. Optics express, 2015. 23(8): p. 9753-9761.
20. Chen, S., et al., Polarization insensitive and omnidirectional broadband near perfect planar metamaterial absorber in the near-infrared regime. Applied Physics Letters, 2011. 99(25): p. 253104.
21. Ding, F., et al., Broadband near-infrared metamaterial absorbers utilizing highly lossy metals. Scientific reports, 2016. 6(1): p. 1-9.
22. Arik, K., et al., Design of mid-infrared ultra-wideband metallic absorber based on circuit theory. Optics Communications, 2016. 381: p. 309-313.
23. Cui, Y., et al., Ultrabroadband light absorption by a sawtooth anisotropic metamaterial slab. Nano letters, 2012. 12(3): p. 1443-1447.
24. Feng, Q., et al., Engineering the dispersion of metamaterial surface for broadband infrared absorption. Optics Letters, 2012. 37(11): p. 2133-2135.
25. Arik, K., S. AbdollahRamezani, and A. Khavasi, Polarization insensitive and broadband terahertz absorber using graphene disks. Plasmonics, 2017. 12(2): p. 393-398.
26. Chen, D., et al., Section 1Tunable broadband terahertz absorbers based on multiple layers of graphene ribbons. Scientific reports, 2017. 7(1): p. 1-8.
27. Khavasi, A., Design of ultra-broadband graphene absorber using circuit theory. JOSA B, 2015. 32(9): p. 1941-1946.
28. Zang, X., et al., Ultra-broadband terahertz absorption by exciting the orthogonal diffraction in dumbbell-shaped gratings. Scientific reports, 2015. 5: p. 8901.
29. Wang, F., et al., Dual-band tunable perfect metamaterial absorber based on graphene. Applied optics, 2018. 57(24): p. 6916-6922.
30. Andryieuski, A. and A.V. Lavrinenko, Graphene metamaterials based tunable terahertz absorber: effective surface conductivity approach. Optics express, 2013. 21(7): p. 9144-9155.
31. Bolotin, K.I., et al., Ultrahigh electron mobility in suspended graphene. Solid-state communications, 2008. 146(9-10): p. 351-355.
32. Zhao, H., et al., Terahertz wavefront manipulating by double-layer graphene ribbons metasurface. Optics Communications, 2017. 402: p. 523-526.
33. Vakil, A. and N. Engheta, Transformation optics using graphene. Science, 2011. 332(6035): p. 1291-1294.
34. Hanson, G.W., Dyadic Green's functions for an anisotropic, non-local model of biased graphene. IEEE Transactions on antennas and propagation, 2008. 56(3): p. 747-757.
35. Morozov, S., et al., Giant intrinsic carrier mobilities in graphene and its bilayer. Physical review letters, 2008. 100(1): p. 016602.
36. Hanson, G.W., Dyadic Green's functions and guided surface waves for a surface conductivity model of graphene. Journal of Applied Physics, 2008. 103(6): p. 064302.

Figures

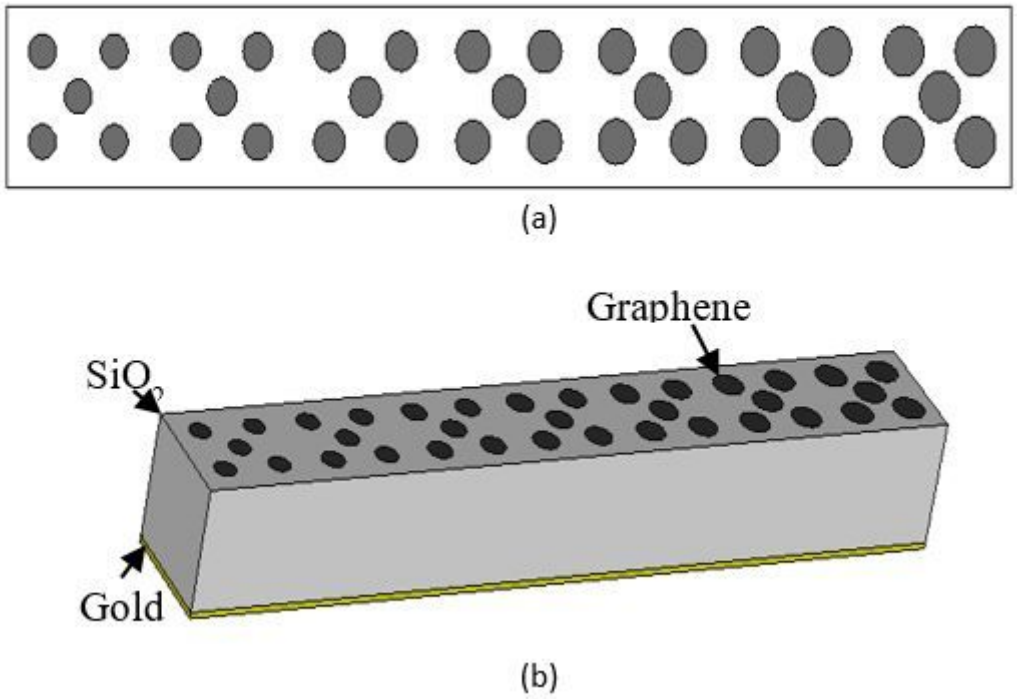

Figure 1

(a) 7 sets of 5 disks. In 1st set, the radius is 400nm. In 2nd is 431nm. In 3rd is 461nm. In 4th is 493nm. In 5th is 525nm. In 6th is 556nm. In 7th is 586nm. (b) Schematic illustration of proposed THz metamaterial absorber. The top layer is composed of graphene disks. The middle layer is SiO2 and the bottom layer is gold.

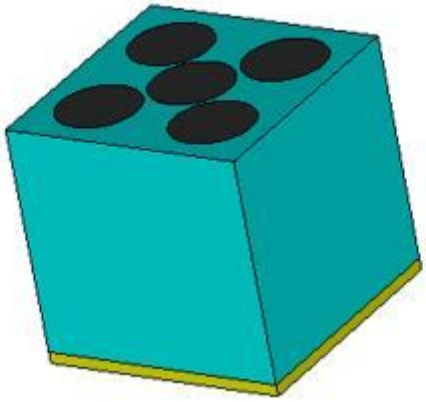

Figure 2

Unit cell with 5 disks of single-layer graphene at top. The middle layer is SiO2 and the bottom layer is gold.

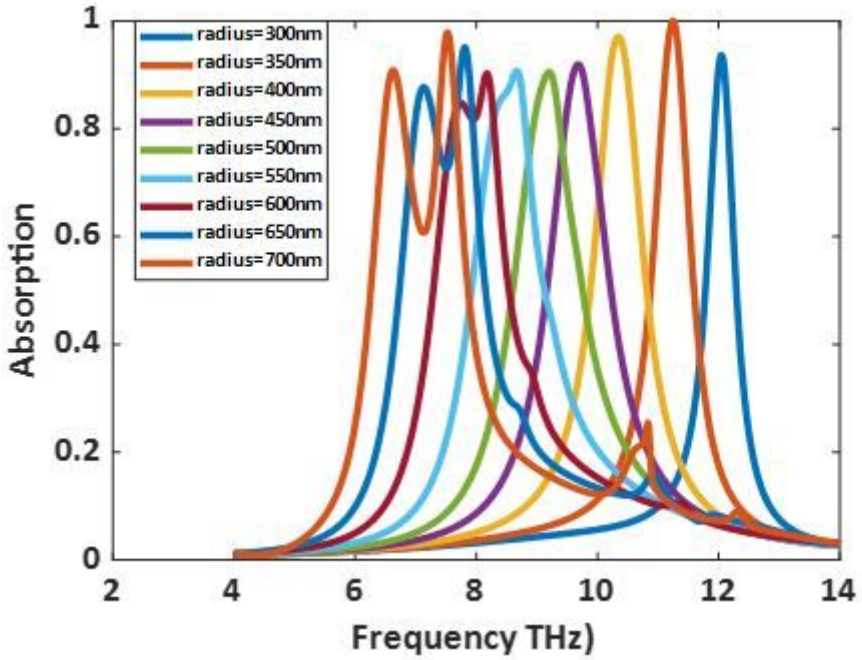

Figure 3

Radius sweep from 300 to 700.

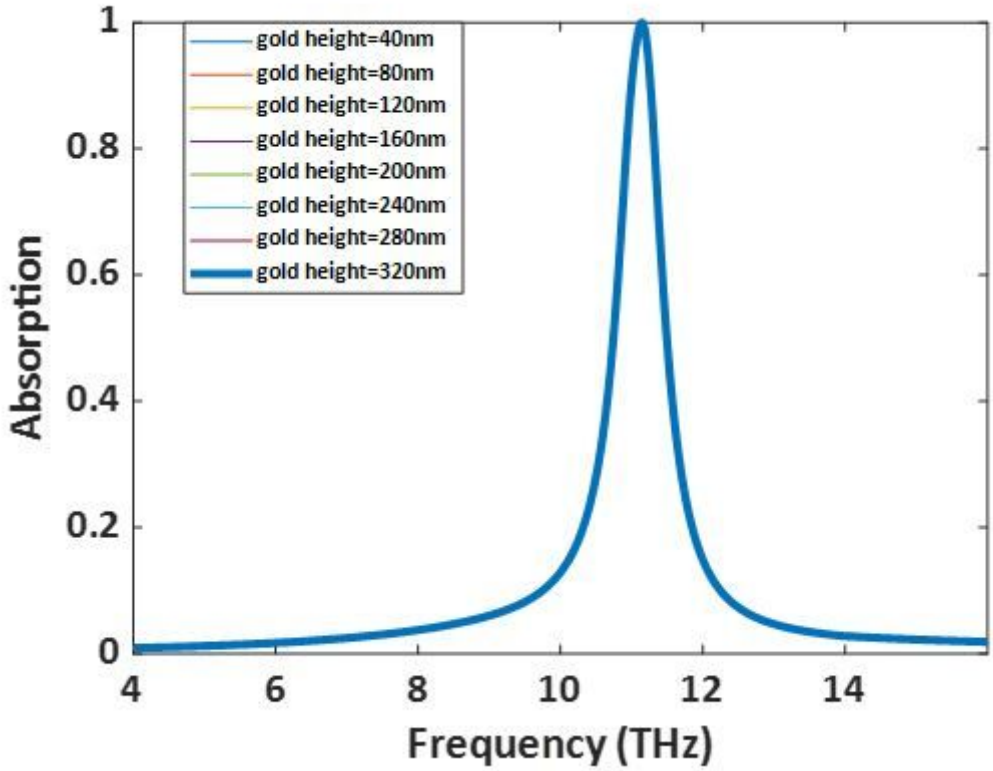

Figure 4

Gold layer height sweep from 40nm to 320nm.

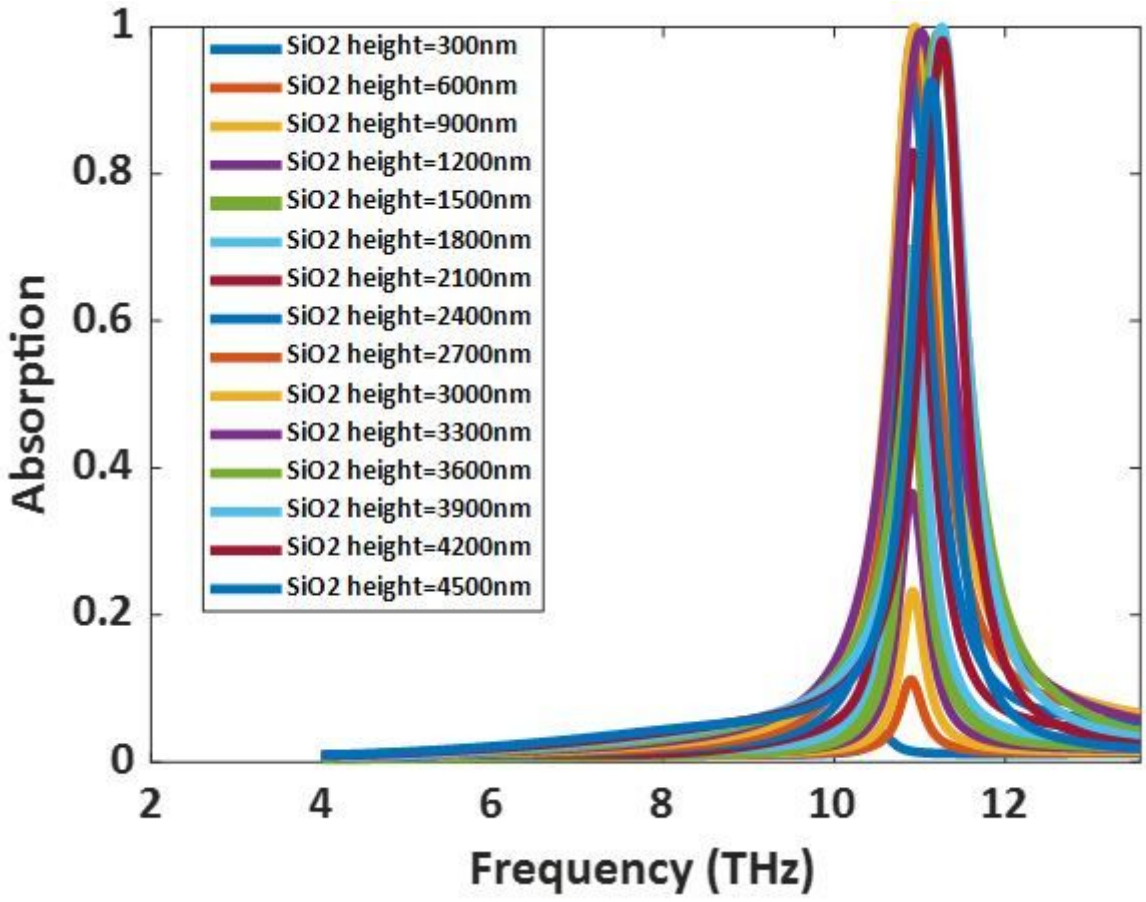

Figure 5

SiO2 layer height sweep from 300nm to 4500nm.

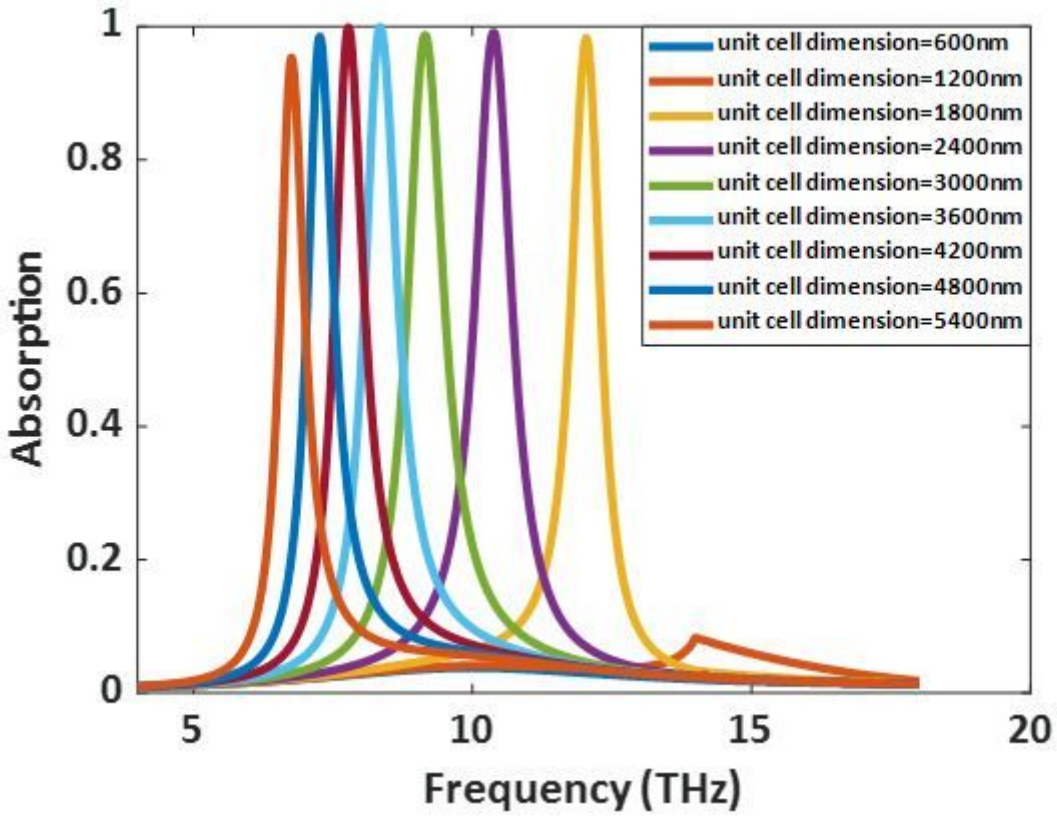

Figure 6

Sweeping the dimension of the unit cell from 600 to 5400nm.

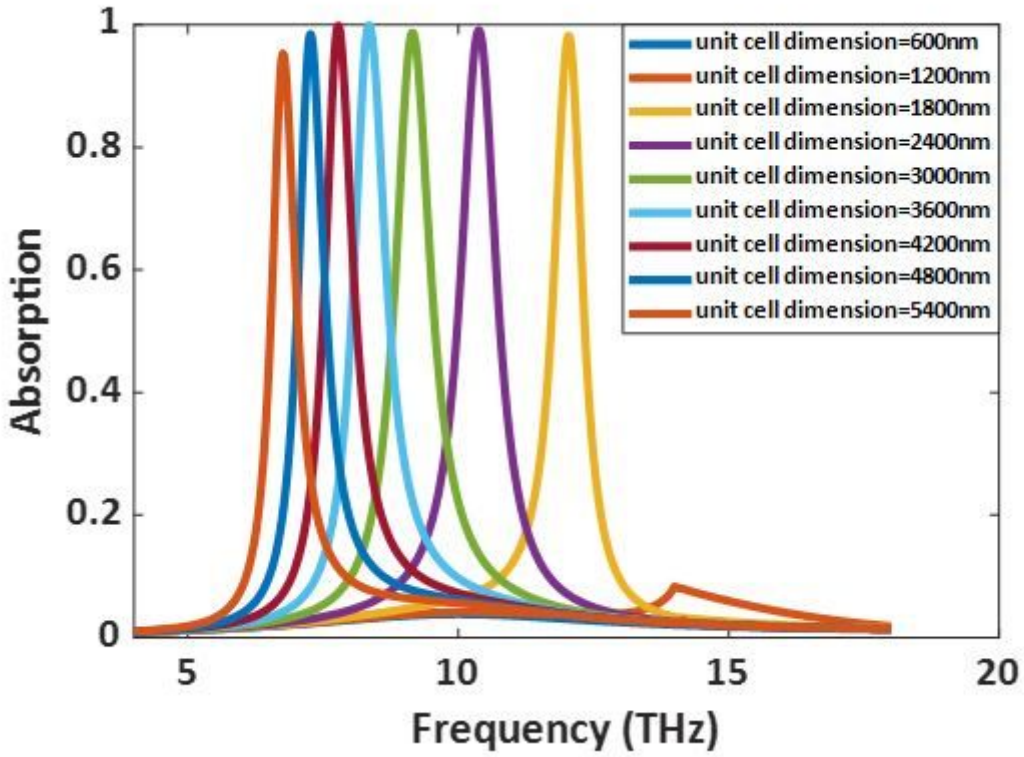

Figure 7

Sweeping the dimension of the unit cell from 700 to 5600nm.

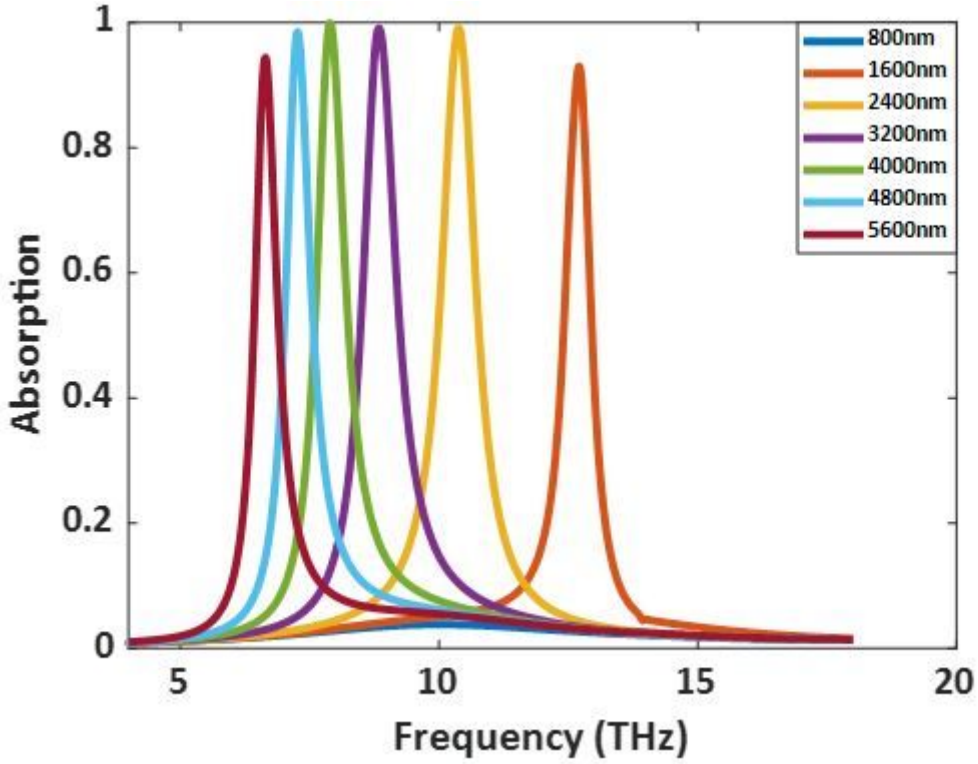

Figure 8

Sweeping the dimension of the unit cell from 800 to 5600nm.

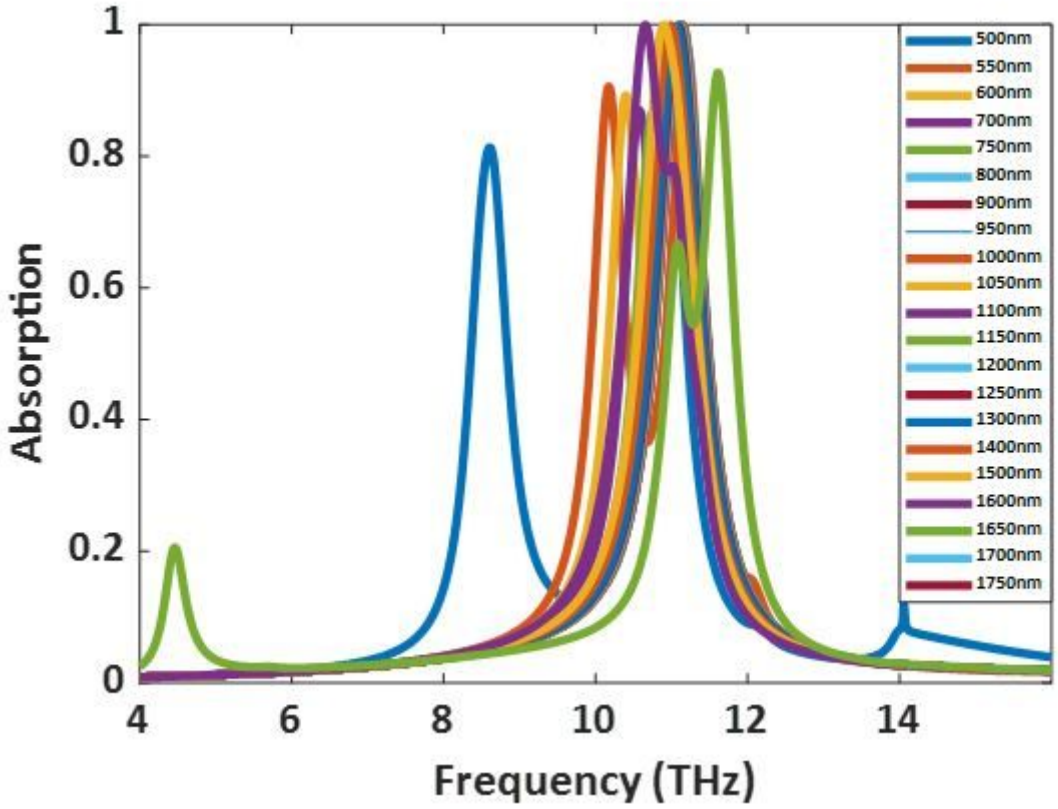

Figure 9

Sweeping the location of disks from 500 to 1750nm.

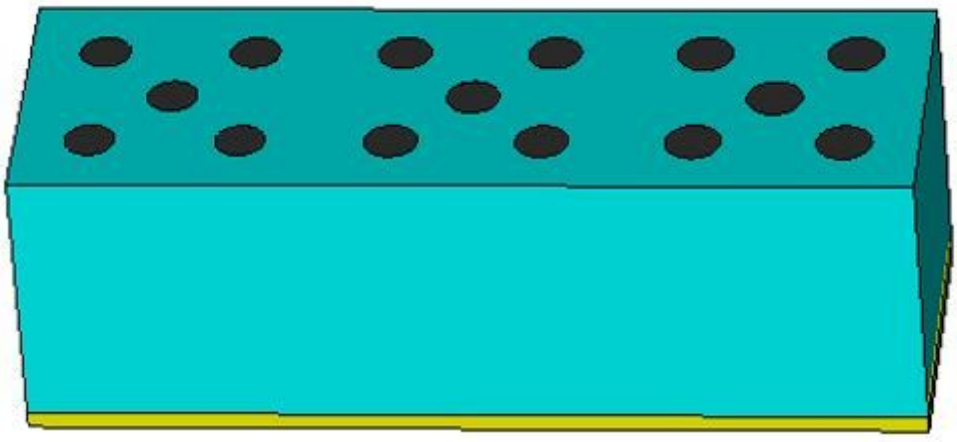

Figure 10

putting 3 unit cells beside each other.

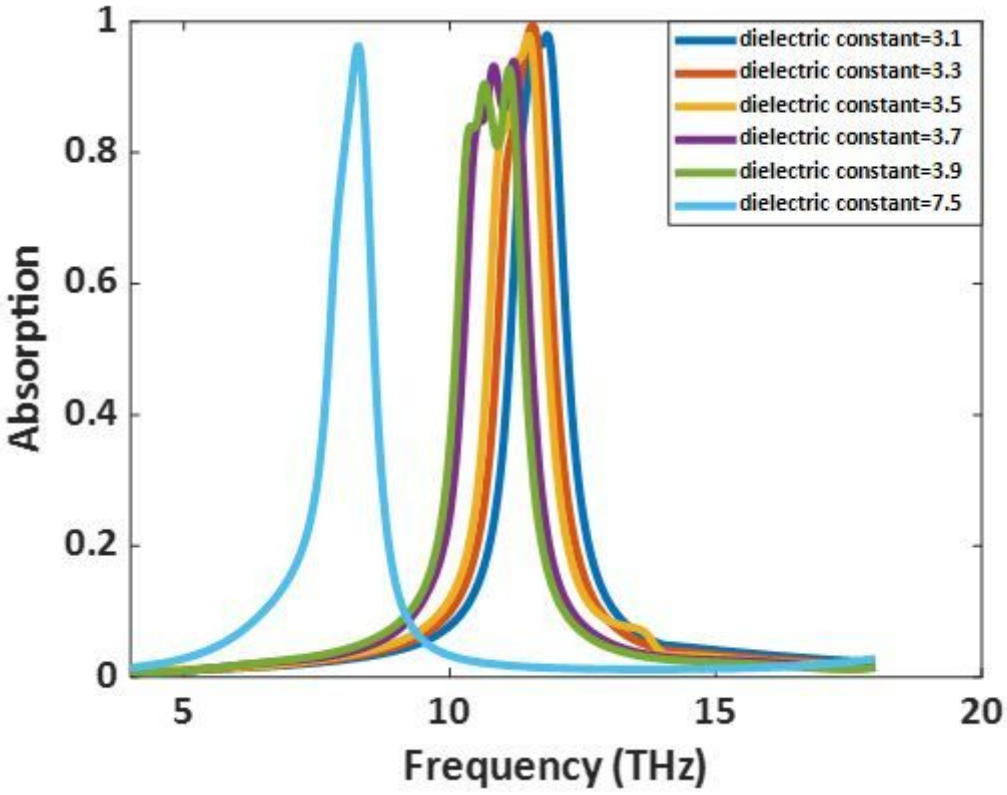

Figure 11

Radii of graphene disks in first unit cell=350nm, second=375nm, and third=400nm with middle layer dielectric constant=3.1 (Rubber), 3.3 (Zircon), 3.5 (Polyimide), 3.7 (Quartz), 3.9 (SiO_2), and 7.5 (Si_3N_4).

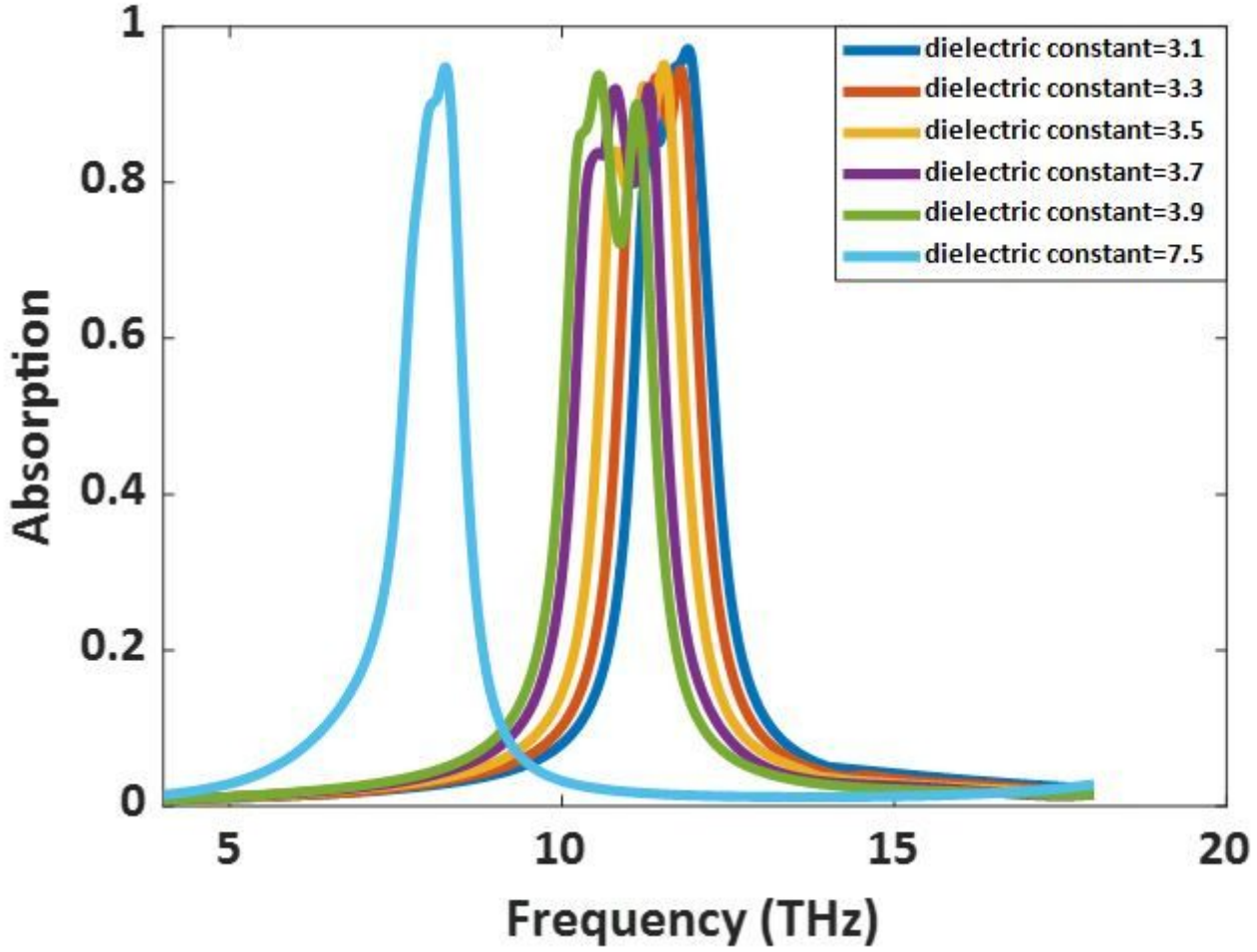

Figure 12

Radii of graphene disks in first unit cell=350nm, second=370nm, and third=390nm with middle layer dielectric constant=3.1 (Rubber), 3.3 (Zircon), 3.5 (Polyimide), 3.7 (Quartz), 3.9 (SiO2), and 7.5 (Si3N4).

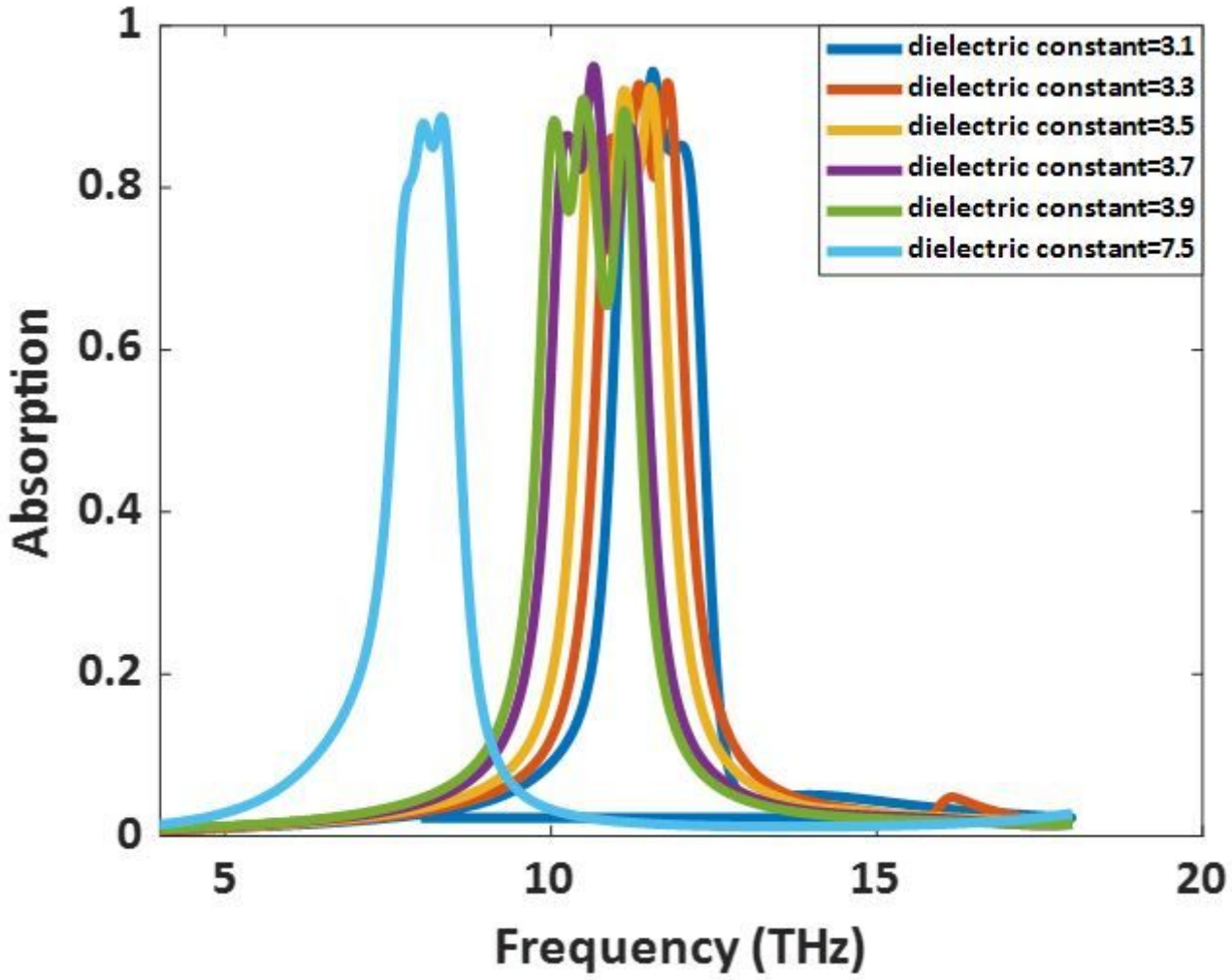

Figure 13

Radii of graphene disks in first unit cell=350nm, second=375nm, and third=400nm with middle layer dielectric constant=3.1 (Rubber), 3.3 (Zircon), 3.5 (Polyimide), 3.7 (Quartz), 3.9 (SiO_2), and 7.5 (Si_3N_4).

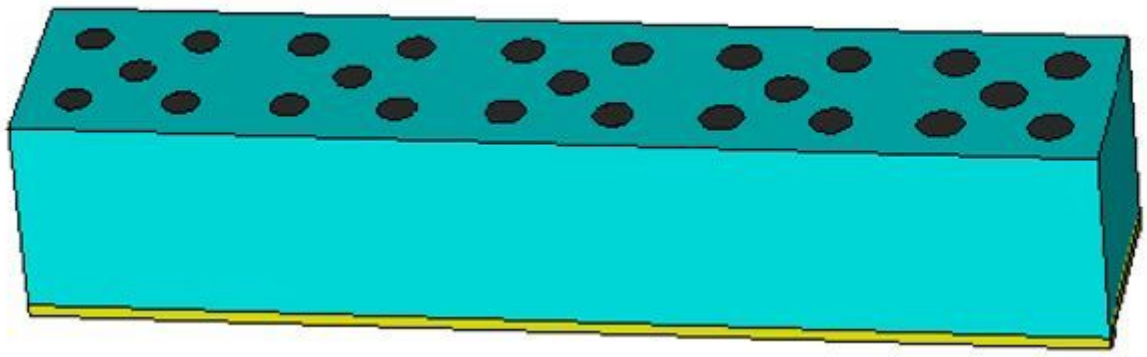

Figure 14

putting 5 unit cells beside each other.

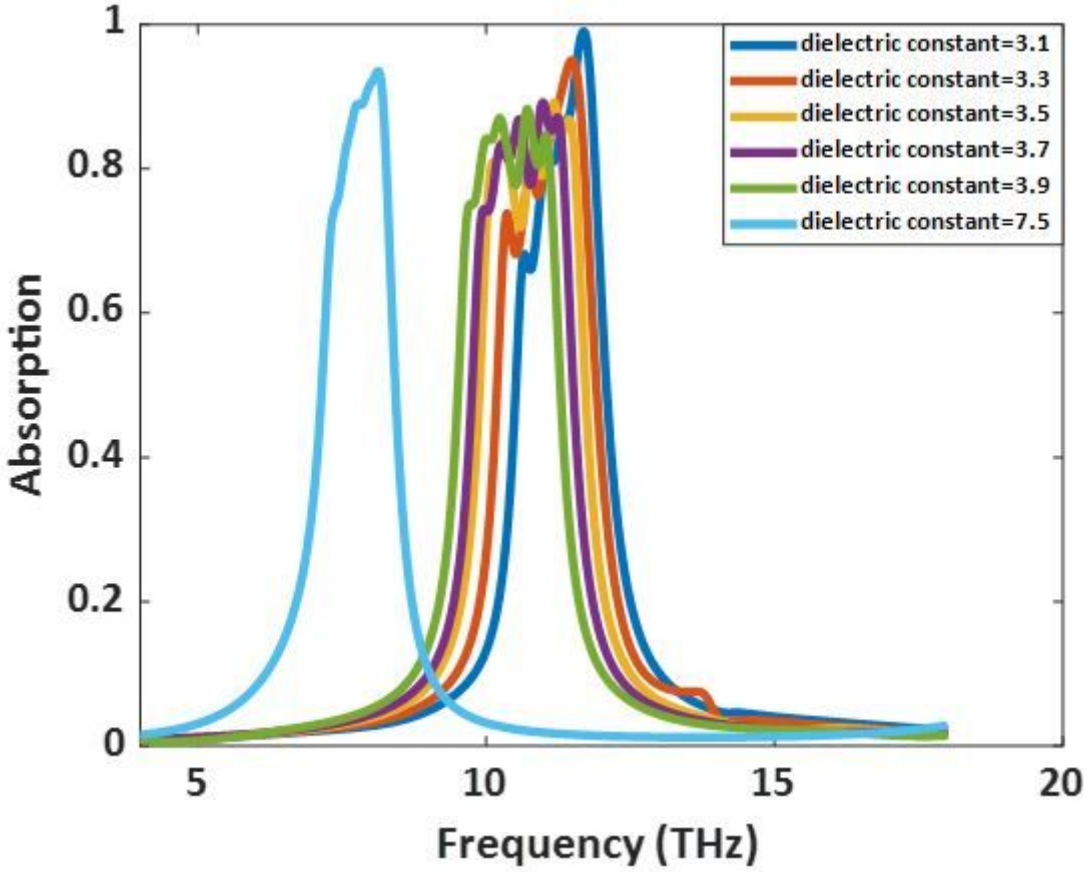

Figure 15

Radii of graphene disks in first unit cell=350nm, second=370nm third=390nm, fourth=410nm and fifth=430nm with middle layer dielectric constant=3.1 (Rubber), 3.3 (Zircon), 3.5 (Polyimide), 3.7 (Quartz), 3.9 (SiO_2) and 7.5 (Si_3N_4).

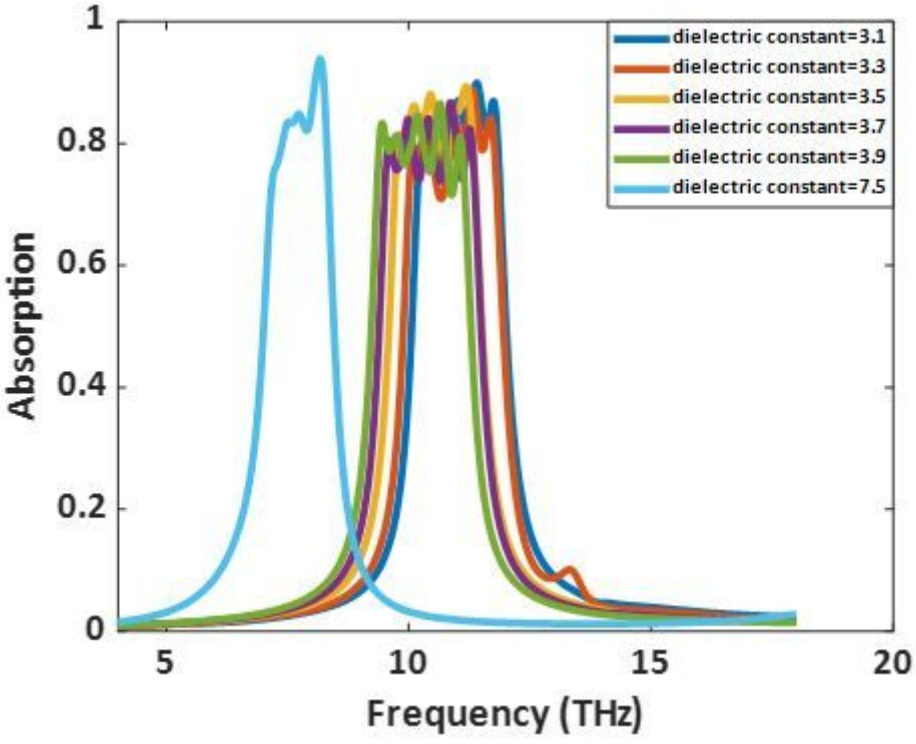

Figure 16

Radii of graphene disks in first unit cell=350nm, second=375nm third=400nm, fourth=425nm and fifth=450nm with middle layer dielectric constant=3.1 (Rubber), 3.3 (Zircon), 3.5 (Polyimide), 3.7 (Quartz), 3.9 (SiO2) and 7.5 (Si3N4).

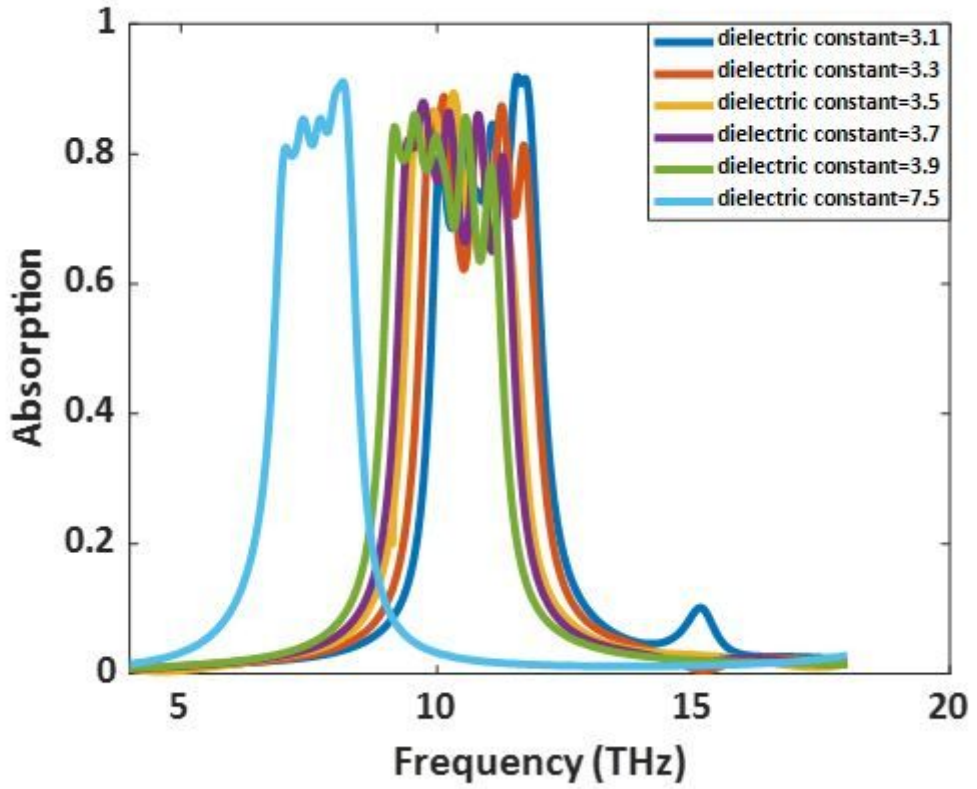

Figure 17

Radii of graphene disks in first unit cell=350nm, second=380nm third=410nm, fourth=440nm and fifth=470nm with middle layer dielectric constant=3.1 (Rubber), 3.3 (Zircon), 3.5 (Polyimide), 3.7 (Quartz), 3.9 (SiO2) and 7.5 (Si3N4).

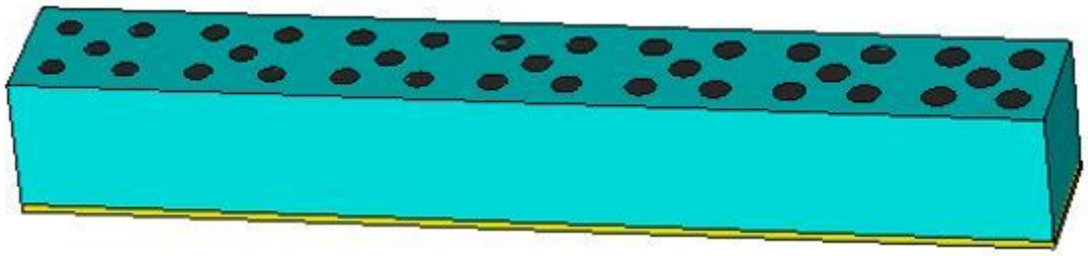

Figure 18

putting 5 unit cells beside each other.

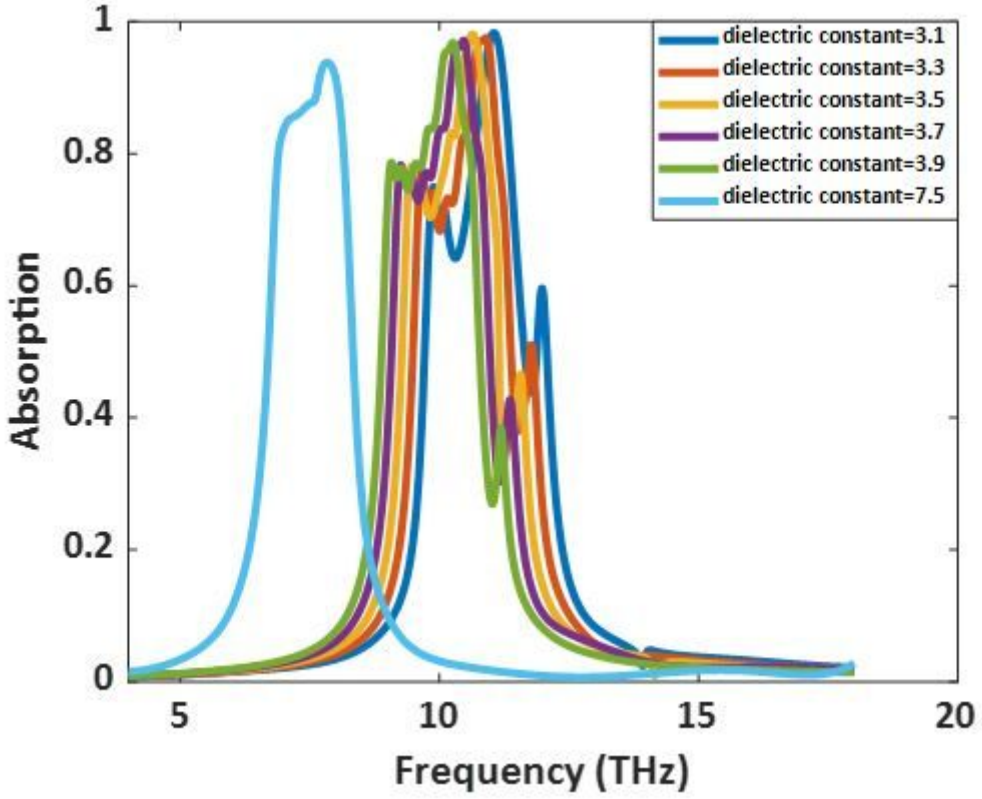

Figure 19

Radii of graphene disks in first unit cell=350nm, second=370nm third=390nm, fourth=410nm, fifth=430nm, sixth=450 and seventh=470 with middle layer dielectric constant=3.1 (Rubber), 3.3 (Zircon), 3.5 (Polyimide), 3.7 (Quartz), 3.9 (SiO_2) and 7.5 (Si_3N_4).

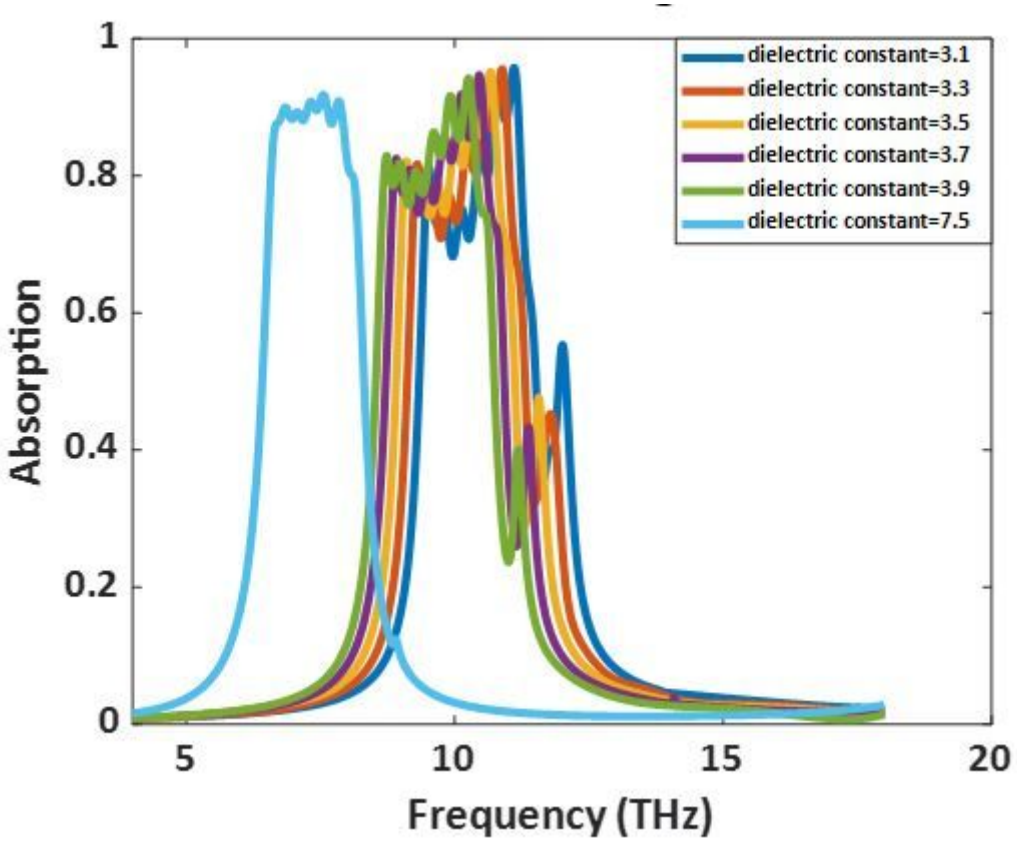

Figure 20

Radii of graphene disks in first unit cell=350nm, second=375nm third=400nm, fourth=425nm, fifth=450nm, sixth=475 and seventh=500 with middle layer dielectric constant=3.1 (Rubber), 3.3 (Zircon), 3.5 (Polyimide), 3.7 (Quartz), 3.9 (SiO_2) and 7.5 (Si_3N_4).

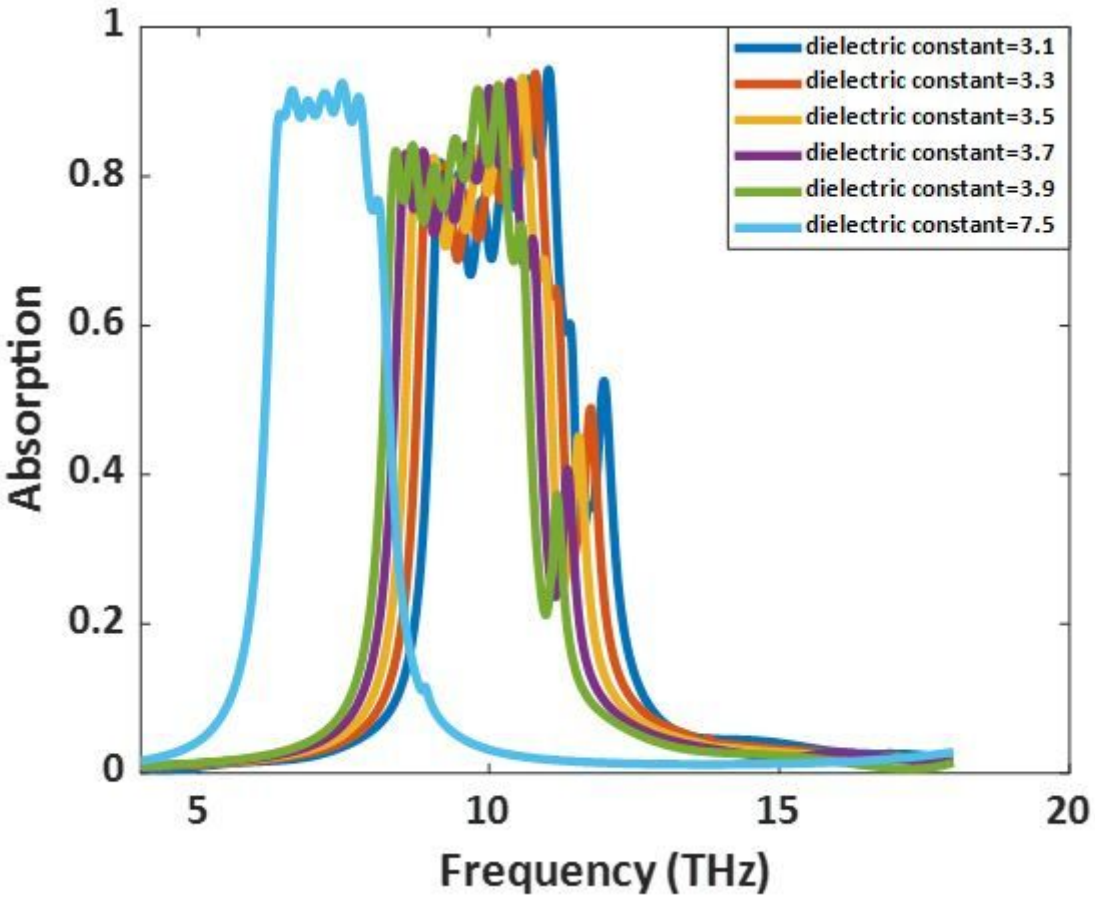

Figure 21

Radii of graphene disks in first unit cell=350nm, second=380nm third=410nm, fourth=440nm, fifth=470nm, sixth=500 and seventh=530 with middle layer dielectric constant=3.1 (Rubber), 3.3 (Zircon), 3.5 (Polyimide), 3.7 (Quartz), 3.9 (SiO_2) and 7.5 (Si_3N_4).

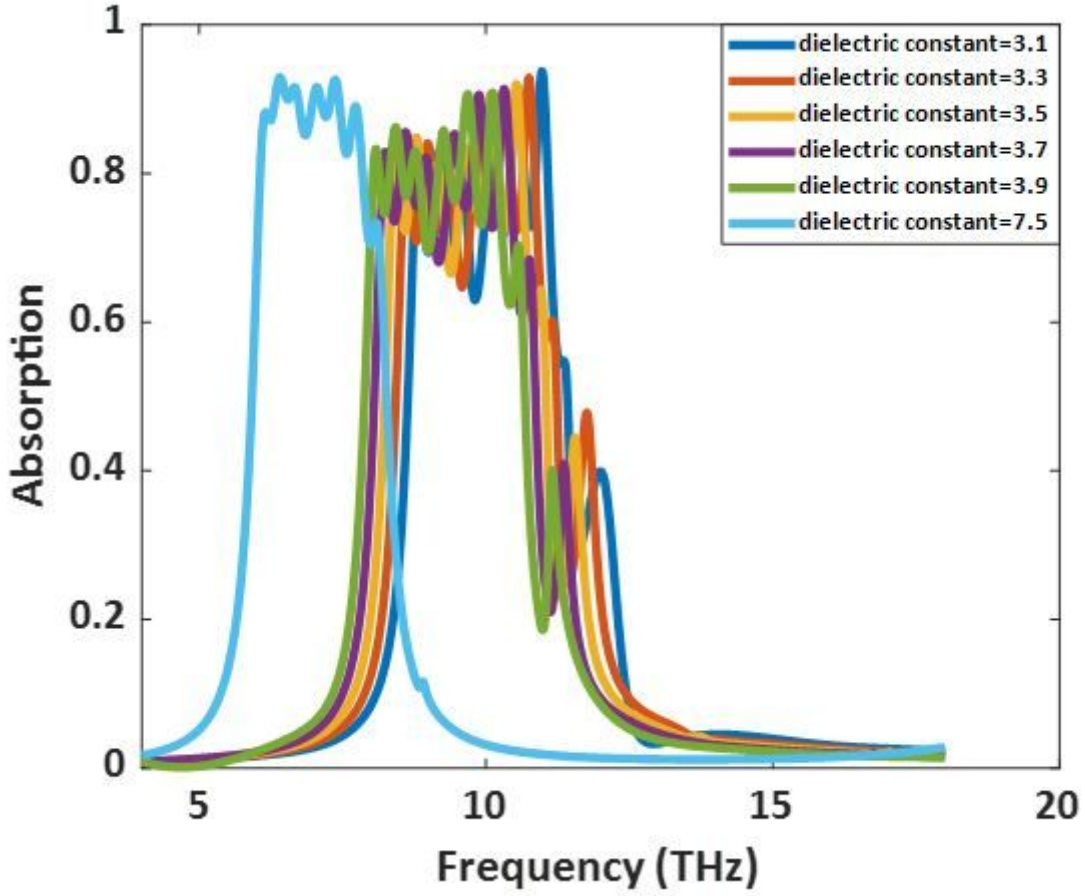

Figure 22

Radii of graphene disks in first unit cell=350nm, second=385nm third=420nm, fourth=455nm, fifth=490nm, sixth=525 and seventh=560 with middle layer dielectric constant=3.1 (Rubber), 3.3 (Zircon), 3.5 (Polyimide), 3.7 (Quartz), 3.9 (SiO_2) and 7.5 (Si_3N_4).

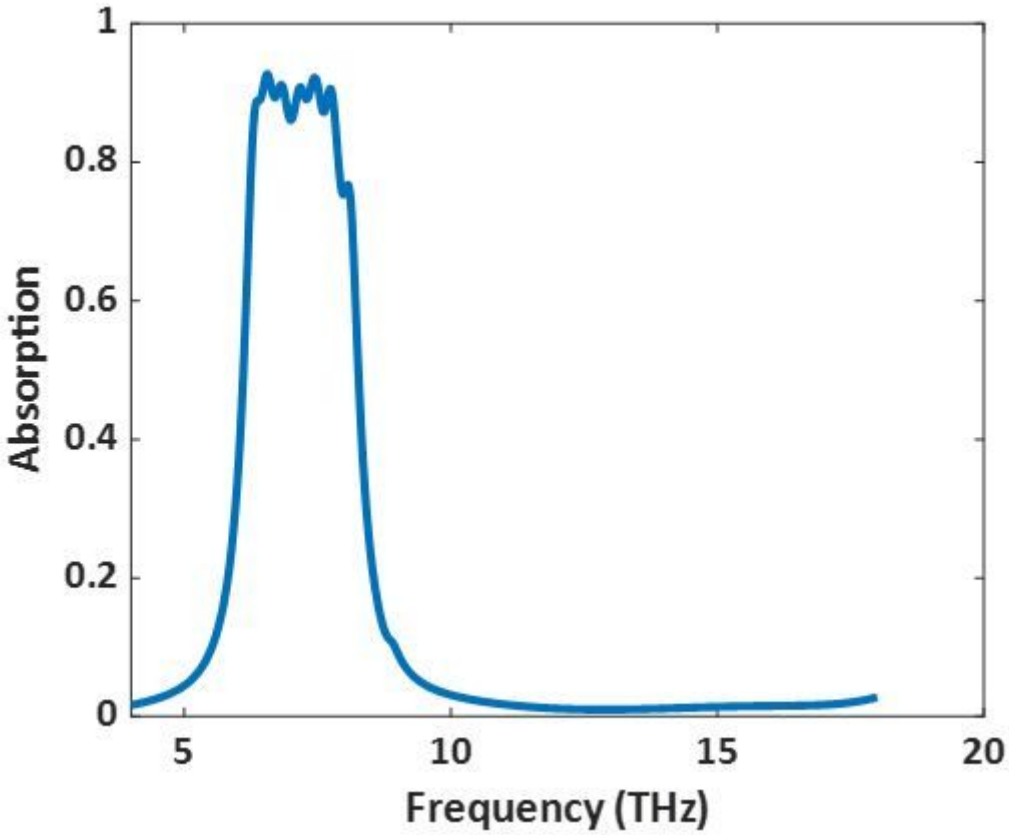

Figure 23

Radii of graphene disks in first unit cell=350nm, second=380nm third=411nm, fourth=443nm, fifth=475nm, sixth=506 and seventh=536 with middle layer dielectric constant= 7.5 (Si3N4).

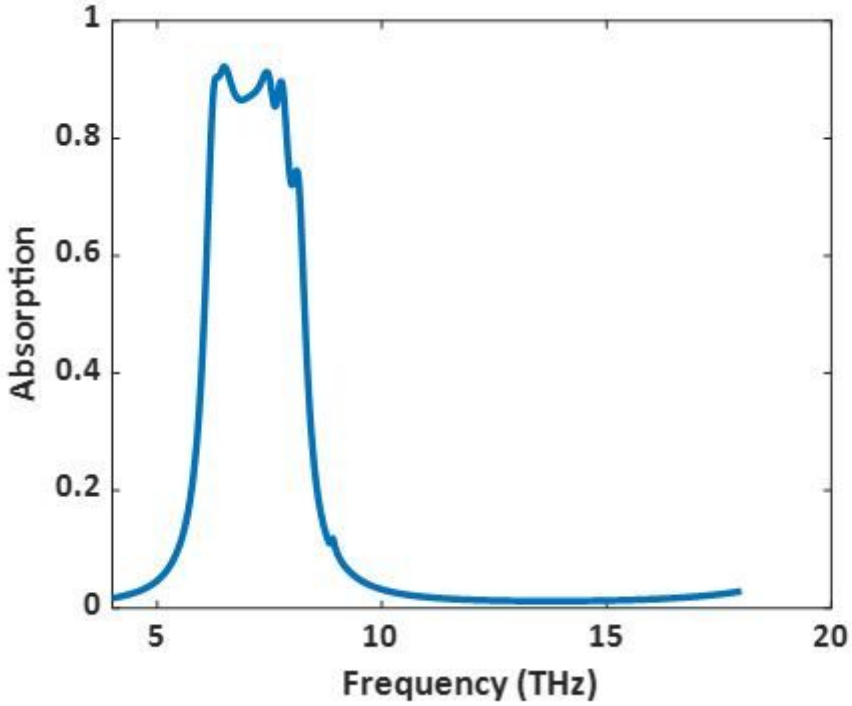

Figure 24

Radii of graphene disks in first unit cell=350nm, second=380nm third=412nm, fourth=446nm, fifth=480nm, sixth=512 and seventh=542 with middle layer dielectric constant= 7.5 (Si3N4).

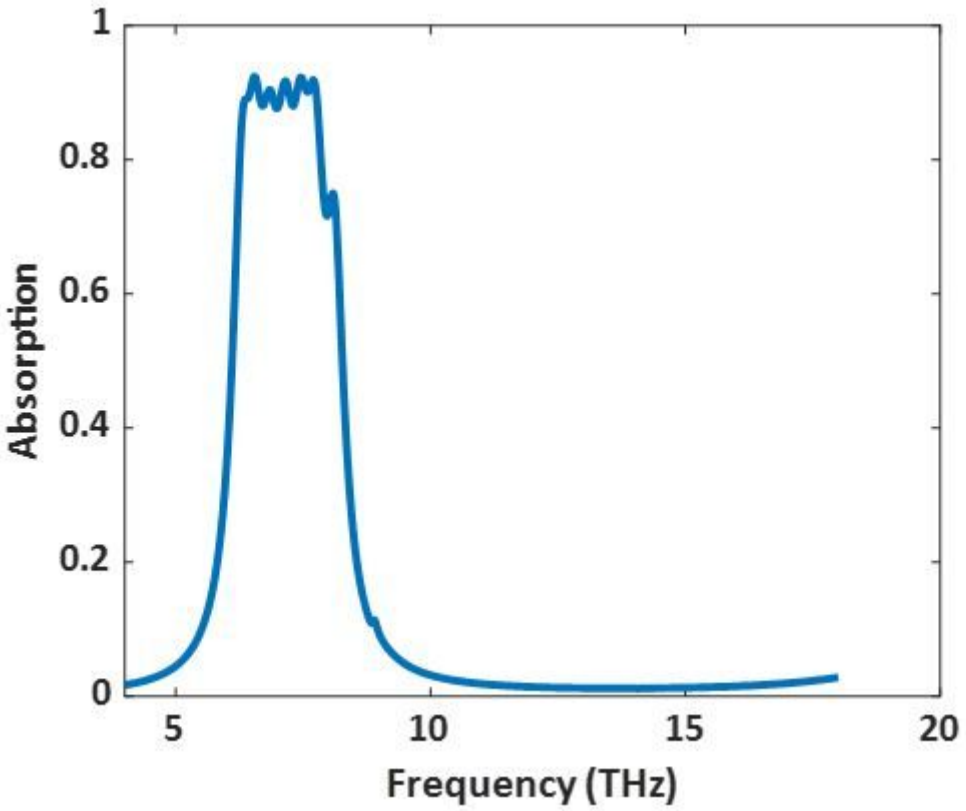

Figure 25

Radii of graphene disks in first unit cell=350nm, second=381nm third=412nm, fourth=443nm, fifth=474nm, sixth=505 and seventh=536 with middle layer dielectric constant= 7.5 (Si3N4).

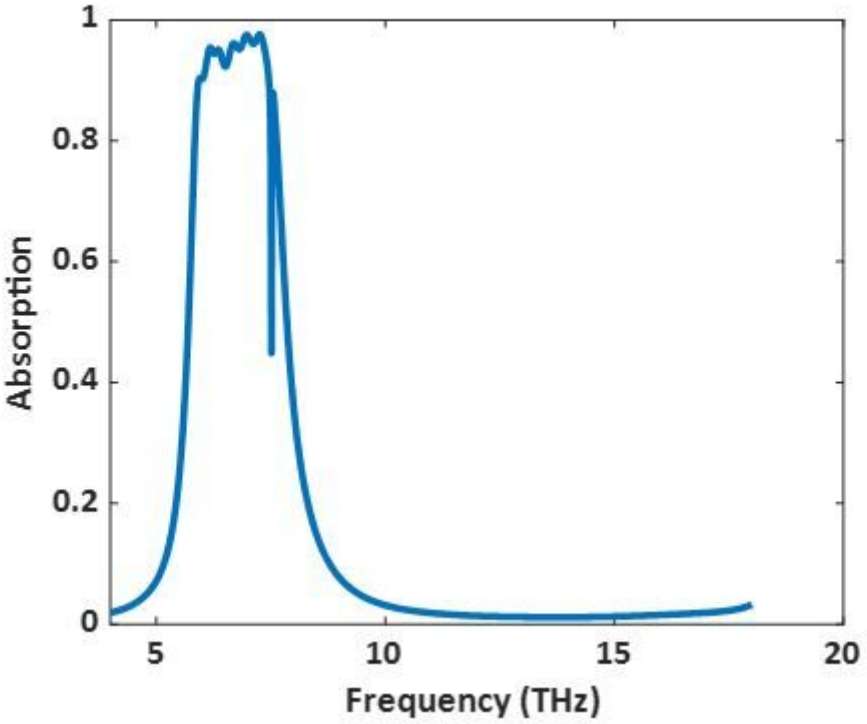

Figure 26

Radii of graphene disks in first unit cell=400nm, second=430nm third=461nm, fourth=493nm, fifth=525nm, sixth=556 and seventh=586 with middle layer dielectric constant= 7.5 (Si3N4).

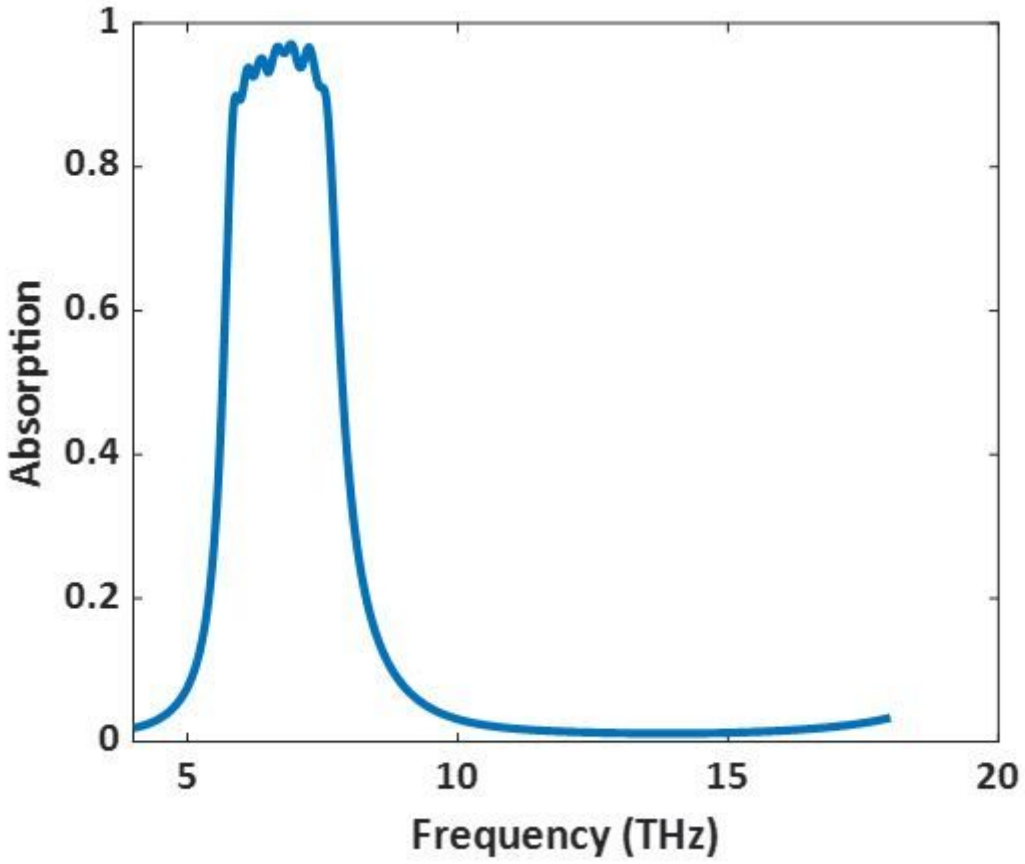

Figure 27

Radii of graphene disks in first unit cell=400nm, second=431nm third=463nm, fourth=496nm, fifth=529nm, sixth=561 and seventh=592 with middle layer dielectric constant= 7.5 (Si3N4).

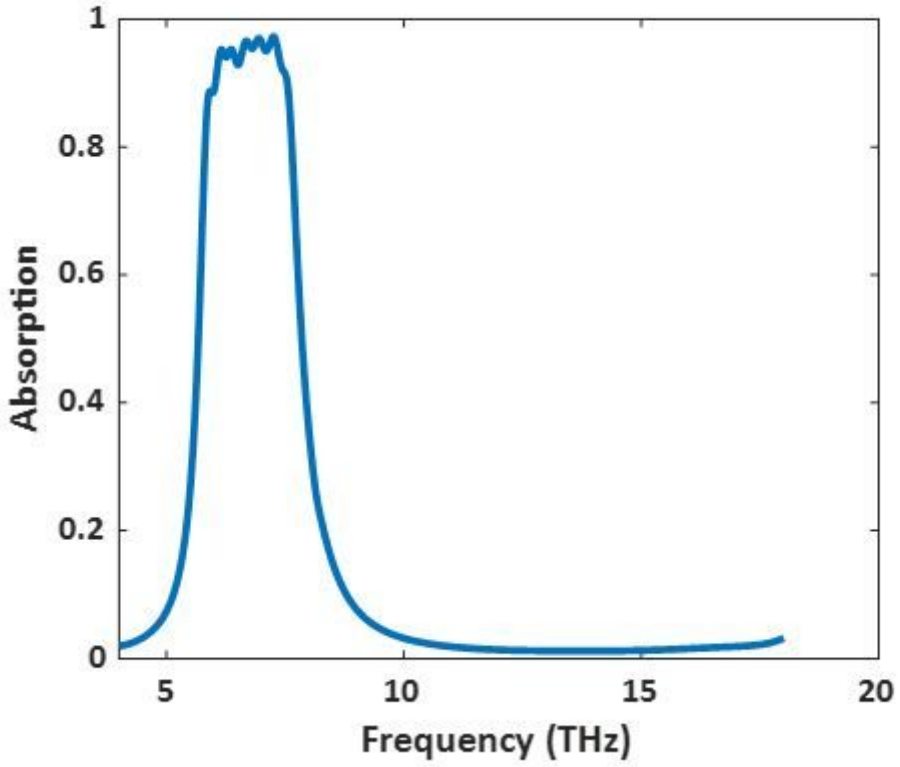

Figure 28

Radii of graphene disks in first unit cell=400nm, second=431nm third=463nm, fourth=495nm, fifth=527nm, sixth=559 and seventh=590 with middle layer dielectric constant= 7.5 (Si3N4).

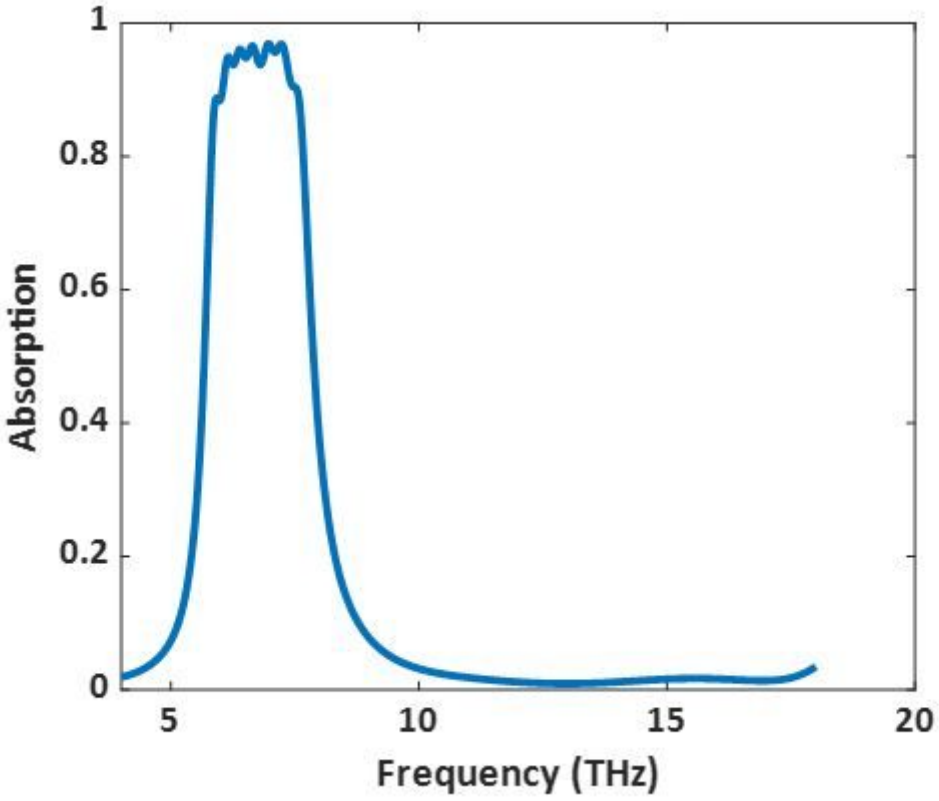

Figure 29

Radii of graphene disks in first unit cell=400nm, second=431nm third=463nm, fourth=495nm, fifth=526nm, sixth=558 and seventh=590 with middle layer dielectric constant= 7.5 (Si3N4).

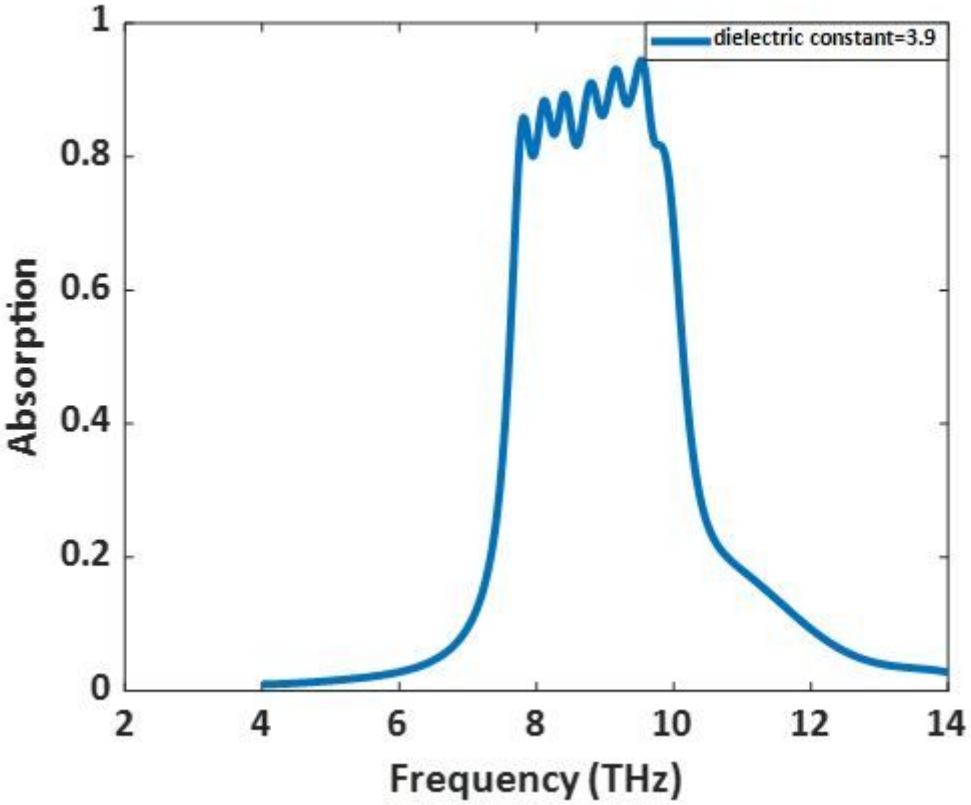

Figure 30

Radii of graphene disks in first unit cell=400nm, second=430nm third=461nm, fourth=493nm, fifth=525nm, sixth=556 and seventh=586 with middle layer dielectric constant= 3.9 (SiO2).